

Michigan Institute for Plasma Science and Engineering (MIPSE) 15th ANNUAL GRADUATE STUDENT SYMPOSIUM

November 20, 2024 University of Michigan North Campus, Ann Arbor, MI 48109

Schedule

I. Special MIPSE Seminar

Johnson Rooms, 3213 Lurie Engineering Center, 1221 Beal Avenue

1:00 – 1:20 pm	Registration, light lunch				
1:20 – 1:25 pm	Prof. Mark J. Kushner, University of Michigan				
	Director, MIPSE				
	Opening remarks				
1:25 – 1:30 pm	Prof. Gozde Tutuncuoglu, Wayne State University				
	Chair, AVS Michigan Chapter				
	Introducing American Vacuum Society Michigan Chapter				
	and Student Chapter				
1:30 – 2:30 pm	Prof. Peter Bruggeman, University of Minnesota				
	Winner, University of Michigan Plasma Prize 2023				
	Low Temperature Plasma Science to Advance Human Health and Enable a				
	Sustainable Future				

II. Poster Presentations

Atrium, **EECS Building**, 1301 Beal Avenue

5:45 – 6:00 pm	Best Presentation Award ceremony
5:30 – 5:45 pm	Poster removal
4:45 – 5:30 pm	Poster Session III
4:00 – 4:45 pm	Poster Session II
3:15 – 4:00 pm	Poster Session I
2:45 – 3:15 pm	Poster setup

Participating institutions: University of Michigan, Michigan State University.

Poster Session I

1-01	Chenyao Huang	U-M	Effect of Secondary Electron Emission on Surface Charging during Plasma Etching for Microelectronics Fabrication
1-02	Andre Antoine	U-M	Characterization of Non-Thermal Phase Transitions in MgO and NaCl with Two-color Ultrashort X-ray Pulses
1-03	Lucas Babati	U-M	Calculating Transport Coefficients in Warm Dense Matter with the Strongly Coupled Transport (SCOUT) Code
1-04	Md Arifuzzaman Faisal	MSU	Enhanced Spatial Growth and Interaction Impedance in Smith-Purcell Radiation with Flattened Dispersion Curves
1-05	Kimberly Beers	U-M	Investigation of Co-Evaporated Bi₂Te₃ Thin Films on HD-4110 Polyimide for use in Thermoelectric Micro-Generators
1-06	Declan Brick	U-M	Model Based Investigation of Parallel Heat Flux in Hall Thrusters
1-07	Khalil Bryant	U-M	Using AWSoM Simulations to Compare to Laboratory Experiments
1-08	Sarah Frechette Roberts	MSU	Extended Hydrogen Plasma Etching of (100) Single Crystal Diamond to Improve MPACVD Growth Quality
1-09	Veronica Contreras	U-M	Channel Formation and Transverse Ion Acceleration from High-Intensity Laser Interactions with Underdense Plasma on OMEGA EP
1-10	Vivian Cribb	U-M	Solar Wind Drivers of Auroral Omega Bands
1-11	Connor DiMarco	U-M	High Energy Particle Measurements at Geostationary Orbit and their Relationship with Omega Band Formation
1-12	Adam Bedel	U-M	Stability Analysis of Dynamic Screw-Pinch Driven Thin-Foil Liner Implosions
1-13	James Welch	U-M	Molecular Dynamics Simulations of Temperature Relaxation Rates for Strongly Magnetized, Ion-Electron, Antimatter Plasmas
1-14	Sheng Lee	MSU	Generation of Ordered Atomic Gold Nanowires via Tipenhanced Terahertz Field
1-15	Tanvi Nikhar	MSU	Effect of Gas Temperature on the Chemical Vapor Deposition of Nanodiamond
1-16	Jisu Jeon	U-M	Dissociation Reaction Sources on Liquid Surfaces and PFAS Removal
1-17	Madison Allen	U-M	Optimal Experimental Design for 2D Electron Measurements in a Hall Effect Thruster Channel

Poster Session II

2-01	Ari Eckhaus	U-M	Experimental Investigation into the Role of Wall Materials in Electron Cyclotron Resonance Magnetic Nozzle Thrusters		
2-02	Abstract withdrawn				
2-03	Yves Heri	MSU	Space-Charge Induced Distortion of Short-Pulse Beams in a Vacuum Drift Space		
2-04	Sarah Feldman	U-M	Hydrogen Sensor via Plasma Techniques Development		
2-05	Yifan Gui	U-M	Onset of Silicon Nanoparticle Crystallinity in Nonthermal Plasmas		
2-06	Md. Mashrafi	MSU	Two-Frequency RF Fields Induced Multipactor in Coaxial Transmission Line		
2-07	Michael Hackett	U-M	Development of an "Ion Mode" for SERENA/Strofio, the Low-Energy Neutral Particle Detector onboard BepiColombo		
2-08	Braden Oh	U-M	Carbon Backsputter Mitigation with a Retarding Beam Dump		
2-09	Milos Sretenovic	MSU	Optimization of Substitutional Phosphorus in n-type Diamond		
2-10	Stephen White	MSU	Gauge Conserving Particle Methods that Naturally Satisfy the Involutions of Maxwell's Equations		
2-11	Isaac Huegel	U-M	Radiation Hydrodynamics Simulations of the Photoionized Plasmas in Accretion-powered Objects Experiment on Z		
2-12	Xitong Xu	MSU	Synthesis of Carbon Nanoparticles via RF Plasma Jet in the Atmosphere		
2-13	William Hurley	U-M	Mass Utilization Scaling with Propellant Type in a Magnetically Shielded Hall Thruster		
2-14	Lan Jin	MSU	Influence of Temporal Shapes of Femtosecond Laser Pulses on Photoemission from a Metal Surface		
2-15	Neil Beri	U-M	Effects of Pulse Chirp on the Stability and Efficiency of Plasma Wakefield Photon Acceleration		
2-16	Kwyntero Kelso	U-M	Streak Camera Characterization at the OMEGA-60 Laser Facility		

Poster Session III

3-01	Alexander Cushen	U-M	MHD-AEPIC Coupled Fluid-Kinetic Simulations of Dipolarization Fronts in Mercury's Nightside Magnetosphere
3-02	Julian Kinney	U-M	Bremsstrahlung Emission in Strongly Coupled Plasmas
3-03	Sheng Lee	MSU	Ultrafast Photocarrier Dynamics in CsPbBr₃ Perovskite Microcrystals
3-04	Jarett LeVan	U-M	Bulk Viscosity of Strongly Coupled Plasmas
3-05	Evan Litch	U-M	Pulsed Low Bias Frequencies for High Aspect Ratio Plasma Etching
3-06	Md Wahidur Rahman	MSU	Parametric Analysis of the Beam Kinetic Energy in Linear Beam Devices
3-07	Miron Liu	U-M	Measurements of the Dispersion and Growth Rate of Plasma Waves in the Plume of a Hollow Cathode
3-08	Sudipta Mondal	U-M	Plasma Enhanced Atomic Layer Deposition of Hydrogen Free In₂O₃ Thin Films with High Charge Carrier Mobility
3-09	Bingqing Wang	MSU	Effects of a Series Resistor on Quantum Tunneling Current in a Dissimilar Metal-Insulator-Metal Nanogap
3-10	Aidan Nakhleh	U-M	Investigating Solar Wind Formation and Propagation via Entropy Cross Correlation Analysis
3-11	Bilal Hassan	U-M	Investigation of Plasma Gratings as a Diagnostic for Low Temperature Plasmas
3-12	Parker Roberts	U-M	Characterizing ExB Plasmas with Time-Resolved Thomson Scattering
3-13	Han-Ting Chen	U-M	Maximizing Energy Efficiency in Selective Plasma-Induced Propylene Epoxidation Using Water as the Oxygen Source
3-14	Jaela Whitfield	U-M	Studies of Preheat-induced Mix in MagLIF targets
3-15	Yeon Geun Yook	U-M	Mechanisms for Cryogenic Plasma Etching
3-16	Grace Zoppi	U-M	Fluid Model Performance Predictions of a Coaxial Rotating Magnetic Field Thruster

Abstracts: Poster Session I

Gauge Conserving Particle Methods that Naturally Satisfy the Involutions of Maxwell's Equations*

Andrew Christlieb a, William Sands b, Stephen White a

(a) Michigan State University (christli@msu.edu, whites73@msu.edu)(b) University of Delaware (wsands@udel.edu)

The Yee grid, at the cost of staggering its mesh, satisfies the involutions of Maxwell's equations by its nature, making it one of the best field solvers for particle-in-cell (PIC) methods. In this poster a new PIC method is presented for the Vlasov-Maxwell system that rises to this challenge. Converting the electric and magnetic fields to vector and scalar potentials using the Lorenz gauge, Maxwell's equations become a set of decoupled vector and scalar wave equations on collocated grids, and a non-separable Hamiltonian formulation of the particle update equations is employed over the Newton-Lorentz equation. The wave equations governing the potentials are solved with the Method of Lines Transpose, semi-discretizing in time and solving the resulting boundary value problem. This will first be discretized in time using a backward difference method and solving the boundary value problem using a Green's function, resulting in a first order in time, fifth order in space, and unconditionally stable method [1]. In addition to these advantages, it is equally accurate in its spatial derivatives, meaning all derivatives in the Hamiltonian update equations are as accurate as the fields themselves. Further, a time-consistency property reveals equivalence between the semi-discrete continuity equation and the semi-discrete Lorenz gauge condition, and Gauss' Law following from the semi-discrete Lorenz gauge condition [2]. Finally, this time-consistency property will be explored in a number of other collocated field solvers featuring the second order centered difference scheme, all backward difference schemes, and all diagonally implicit Runge-Kutta schemes [3]. Numerical results will showcase these methods across several experiments.

*This research was supported by AFOSR grants FA9550-19-1-0281 and FA9550-17-1-0394, NSF grant DMS-1912183, and DOE grant DE-SC0023164.

- [1] Christlieb, A. J., Sands, W. A., and White, S. R., A Particle-in-cell Method for Plasmas with a Generalized Momentum Formulation, Part I: Model Formulation, 2024. arXiv: 2208.11291 [physics.plasm-ph].
- [2] Christlieb, A. J., Sands, W. A., and White, S. R. A Particle-in-Cell Method for Plasmas with a Generalized Momentum Formulation, Part II: Enforcing the Lorenz Gauge Condition. J Sci Comput 101, 73 (2024). https://doi.org/10.1007/s10915-024-02728-6.
- [3] Christlieb, A. J., Sands, W. A., and White, S. R., A Particle-in-cell Method for Plasmas with a Generalized Momentum Formulation, Part III: A Family of Gauge Conserving Methods, 2024. arXiv: 2410.18414 [physics.plasm-ph].

Characterization of Non-Thermal Phase Transitions in MgO and NaCl with Two-color Ultrashort X-ray Pulses*

<u>Andre Antoine</u> ^a, Fabien Dorchies ^b Hauke Höppner ^c, Ichiro Inoue ^d, Hae Ja Lee ^e, Nikita Medvedev ^f, Bob Nagler ^e, Jumpei Yamada ^d, Alexander Thomas ^a and Phil Heimann ^e

- (a) University of Michigan, 500 S State St, Ann Arbor, MI (aantoine@umich.edu)
 - (b) Univ. Bordeaux, CNRS, CEA, CELIA, UMR 5107, Talence, France
 - (c) Helmholtz-Zentrum Dresden-Rossendorf, Dresden, Germany
 - (d) RIKEN SPring-8 Center, 1-1-1 Kouto, Sayo, Hyogo, Japan
- (e) Linac Coherent Light Source, SLAC National Accelerator Laboratory, Menlo Park, California, USA
 - (f) Institute of Physics, Czech Academy of Sciences, Na Slovance 1999/2, 182 21 Prague 8, Czech Republic

With x-ray Free Electron Lasers (FEL), intense xray FEL pulses interact with samples, which can alter their electronic and atomic structures [1]. Previous experiments on x-ray FEL-matter interactions have mostly focused on semiconductors like diamond and silicon [2-4]. However, little is known about x-rayinduced bond breaking in multi-element solids or ionic solids. Recent calculations have predicted a crystallineto-disordered phase transition in sodium chloride (NaCl) upon high-intensity x-ray interaction [5]. Using FEL x-ray pump and x-ray probe pulses, we can induce non-thermal phase transitions and detect new material phases. We have investigated the time-dependent intensity of diffraction peaks in NaCl and magnesium oxide (MgO). Our experimental observations are compared with density functional theory and particlein-cell simulations. Our findings reveal the ultrafast responses of these materials, analyzed through the variations in diffraction peak intensities

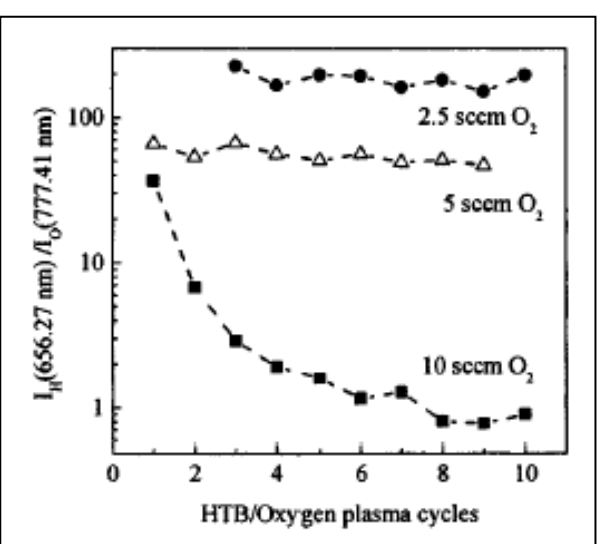


Figure 1 - Captions should be Times New Roman 11 pt font. Figures should be embedded in the text inside a text box. Captions should be under the figure in the same text box as the figure.

*Work supported by the NSF and DOE

- [1] S. Boutet et al., Science 337, 362 (2012).
- [2] I. Inoue et al., Physical Review Letters 126, 117403 (2021).
- [3] I. Inoue et al., Proceeding Nat. Acad. Sciences 113, 1492 (2016).
- [4] N. Hartley et al., High Energy Density Physics 32, 63 (2019).
- [5] R. Voronkov et al., Scientific Reports 10, 13070 (2020).

Calculating Transport Coefficients in Warm Dense Matter with the Strongly Coupled Transport (SCOUT) Code *

Lucas J. Babati ^a, Nathaniel R. Shaffer ^b and Scott D. Baalrud ^a

- (a) Department of Nuclear Engineering and Radiological Sciences, University of Michigan, Ann Arbor, Michigan (Ibabati@umich.edu)
 - (b) Laboratory for Laser Energetics, Rochester, New York

When using a hydrodynamic description of warm dense matter and high energy den- sity plasmas, traditional theories for transport coefficients begin to break down. In this regime, collisions are not determined by binary Coulomb collisions, but instead by many body Coulomb collisions. The Mean Force Kinetic Theory (MFKT) [1] provides an alternate closure to the BBGKY hierarchy based on expanding about a perturbation from equilibrium rather than about strength of correlations and extends plasma theory into the strongly coupled regime. The MFKT produces the same fluid equations as the traditional theories, but with altered trans- port coefficients and equation of state (EOS). Thus, existing fluid codes would only need to update transport and EOS tables. The Strongly Coupled Transport (SCOUT) code is presented which solves for transport coefficients in the warm dense matter regime using a Chapman-Enskog expansion for the MFKT. The MFKT is extended into the WDM regime by including the effects of degenerate electrons, whose screening effect are modeled by the potential of mean force which is obtained using an Average Atom (AA) and Quantum Hyper-Netted Chain (QHNC) model [2]. Additionally, when needed a quantum description of electron scattering is used to calculate cross-sections.

* This material is based upon work supported by the US Department of Energy, National Nuclear Security Administration, under award No. DE-NA0004146 and by the Department of Energy [National Nuclear Security Administration] University of Rochester "National Inertial Confinement Fusion Program" under award No. DE-NA0004144.

- [1] S. D. Baalrud and J. Daligault, Phys. Plasmas 26, 082106 (2019).
- [2] C. E. Starrett and Saumon, HEDP 10, 35-42 (2014).

Enhanced Spatial Growth and Interaction Impedance in Smith-Purcell Radiation with Flattened Dispersion Curves

Md Arifuzzaman Faisal, Peng Zhang

Department of Electrical and Computer Engineering, Michigan State University, East Lansing, MI (pz@egr.msu.edu)

Smith-Purcell radiation (SPR) occurs when charged particles travel near a periodic structure (Fig. 1). SPR has gained significant attention due to its potential applications in various fields, including particle accelerators and terahertz radiation sources [1]. In this study, we investigate the shape of the SPR dispersion curves on SPR growth rate, beam current requirements and output power. Our hot-tube dispersion analysis [2] shows that a flatter dispersion enhances spatial growth rates (Fig. 2) and increases the coupling impedance [3], particularly near the upper band edge [4]. This leads to lower electron beam current requirements for achieving a state of absolute or marginal instability [4]. Higher spatial growth rates or interaction impedance implies a stronger susceptibility to instability and thus SPR at lower beam current. The results will be useful for optimizing SPR device performance through grating parameter (grating height and width) tuning.

* This work was supported by the Office of Naval Research (ONR) YIP Grant No. N00014-20-1-2681, the Air Force Office of Scientific Research

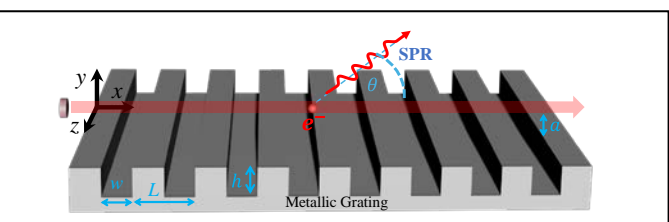


Figure 1 - Schematic of Smith-Purcell grating and beam configuration.

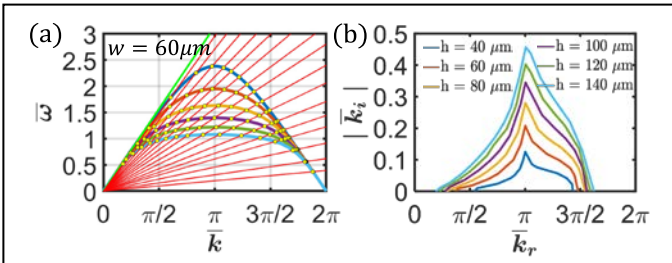


Figure 2 – (a) Cold-tube dispersion relations for different groove height (h=40, 60, 80, 100, 120 and $160 \mu m$) with constant groove width ($w=60 \mu m$), grating period length ($L=120 \mu m$), and beam grating distance ($a=10 \mu m$). The green line represents the light line, and the red lines are the beam lines at different beam energies. (b) Corresponding spatial growth rates at different beam energies (or different normalized wave number).

(AFOSR) Grant No. FA9550-20-1-0409, and Grant No. FA9550-22-1-0523.

- [1] P. Zhang, L. K. Ang, and A. Gover, "Enhancement of coherent Smith-Purcell radiation at terahertz frequency by optimized grating, prebunched beams, and open cavity," Phys. Rev. Spec. Top. Accel. Beams 18, no. 2, p. 020702, Feb. 2015, doi: 10.1103/PhysRevSTAB.18.020702.
- [2] M. A. Faisal and P. Zhang, "Grating Optimization for Smith–Purcell Radiation: Direct Correlation Between Spatial Growth Rate and Starting Current," IEEE Trans. Electron Devices **70**, no. 6, pp. 2860–2863, Jun. 2023, doi: 10.1109/TED.2022.3208846.
- [3] R. Kompfner, "Travelling-wave tubes," Rep. Prog. Phys. **15**, no. 1, p. 275, Jan. 1952, doi: 10.1088/0034-4885/15/1/309.
- [4] F. Antoulinakis, P. Wong, A. Jassem, and Y. Y. Lau, "Absolute instability and transient growth near the band edges of a traveling wave tube," Phys. Plasmas **25**, no. 7, p. 072102, Jul. 2018, doi: 10.1063/1.5028385.

Investigation of Co-Evaporated Bi₂Te₃ Thin Films on HD-4110 Polyimide for use in Thermoelectric Micro-Generators *

<u>Kimberly Beers</u> ^{a,b}, Khalil Najafi ^{a,b}, Adarsh Ravi ^c, Qian Zhang ^c, Baoxing Chen ^c

(a) University of Michigan (kimbeers@umich.edu)(b) Center for Wireless Integrated MicroSensors and Systems (WIMS2)(c) Analog Devices Inc.

Micro-thermoelectric generators (μ TEG) find many applications such as in wearable and internet of things (IoT) devices where continuous, self-powered sensing is required. Thin-film TEGs fabricated have been of special interest because of their smaller size, lower cost, and better flexibility compared to bulk TEGs. Most flexible thin-film TEGs use standard polyimide (PI), Kapton, substrates, which is usually not patterned [1]. Quasi-vertical-lateral TEGs have been fabricated on a Si substrate using patternable PI islands (\sim 5 μ m) to support the thermoelectric (TE) legs [2]. It is desirable to increase this thickness to >20 μ m to improve thermal resistance between the hot and cold sides. Past work also explored the deposition of micron-thick TE thin films on sidewalls of tall (40 μ m) vertical SiO₂ TE legs, thus providing a long TE element [3]. This work investigates co-evaportaed TE films and their properties when deposited on photo-definable PI HD-4110 of varying thickness. HD-4110 is a negative-tone photo-definable PI that can be deposited to \sim 50-60 μ m thick. To our knowledge this PI has not been utilized for TEG films but has several key advantages. It can be patterned with angled sidewalls, withstands high temperatures, and is a robust material that can be used for flexible TEGs. This paper reports preliminary results of the Bi₂Te₃ film quality on HD-4110 films of different thickness, and compares with films deposited on SiO₂.

Measurement of film properties including electrical resistivity, atomic composition, grain size, and Seebeck coefficient have been performed. PI HD-4110 films were spun and cured onto half of 4-inch Si wafers that had a thermally-grown 500nm oxide layer. The other half of each wafer had only the oxide. The cured PI films were 6, 12, and 35 μ m thick. Bi₂Te₃ was deposited by co-evaporation at a temperature of ~260°C to a thickness ~0.9 μ m on all wafers. Atomic composition of the Bi₂Te₃ film was 33:67, Bi:Te. The adhesion of TE films was much better on PI than SiO₂. TE film morphology (grain structure, size, and orientation) did not change substantially with varying PI thickness (thicker PI produced grain sizes that were on average only ~10% larger). TE films deposited on oxide had on average a grain size about 15% smaller than those on PI, and were found to have slightly higher electrical resistivity. Seebeck coefficient was similar on all PI thicknesses and measured to be -172±10 μ V/K. These results are promising for fabrication of quasi-vertical μ TEGs using thin film TE supported by thick PI islands at the end of the text.

- [1] Misra, V., et al., Proceedings of the IEEE. **103**(4), 665–681, (2015).
- [2] B. Chen, P.M. McGuinness, W.A. Lane, J. Cornett, US Patent US9, 748, 466B2.
- [3] Y. Yuan, K. Najafi, Proc. PowerMEMS Conf. W2A-02, 1-5, (2018).

^{*} Work supported by Analog Devices Inc.

Model Based Investigation of Parallel Heat Flux in Hall Thrusters

Declan Brick, Parker Roberts and Benjamin Jorns

University of Michigan, Department of Aerospace Engineering (brickd@umich.edu)

To date, the problem of anomalous transport has precluded predictive modeling of Hall thrusters. That is, an ad-hoc anomalous collision frequency term (ν_{an}) is included in the generalized Ohm's law for models to correctly capture cross-field electron transport. First-principles formulations of ν_{an} have struggled to capture the orders of magnitude drop in the frequency observed in empirical closure profiles. Recently, non-invasive diagnostics have directly measured electron properties, finding ν_{an} profiles with shallower local minimums, as shown in Figure 1, in addition to electron temperatures twice as large as

previously expected. [1] An investigation using the experimental profiles of v_{an} found that models only matched the plasma properties after varying the heat flux and electron losses to the walls, demonstrating that higher temperatures allow for shallower local minimums in the collision frequency profile. [2] While demonstrating the need to investigate the electron energy transport, only a single operating condition and one-dimensional profiles were considered. Thus, we turn to recent measurements of electron properties in other operating conditions and 2D temperature profiles. [3] Notably, this work found that electrons are not isothermal along a field line and the particle density was too low to support a Fourier representation of the heat flux, as previously thought. In this limit, we turn to heat

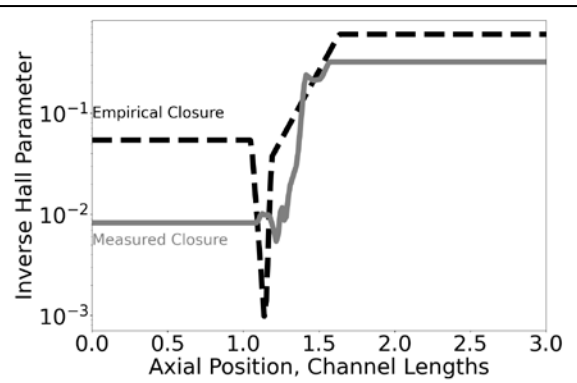


Figure 1 – Comparision between calibrated empircal closure and experimentally measured closue for the H9 Hall thruster operating on krypton at 300V and 15A

flux limiters to understand energy transport in the plasma. [4] A heat flux limiter sets the maximum limit on the heat flux as

$$\vec{q} = \alpha n T \vec{v}$$

where \vec{q} is the heat flux, α is a tunable constant, n is number density, T is temperature, and \vec{v} is velocity. In this work, we apply the heat flux limiter along magnetic field lines and tune the value of α for multiple operating conditions for a 9kW class magnetically-shielded Hall thruster to match plasma properties. These tuned simulations are then investigated for building a greater understanding of electron energy transport in Hall thrusters.

*This work was supported by the Graduate Research Fellowship Program from the National Science Foundation and the NASA Joint Advanced Propulsion Institute. Additional support in part through computational resources and services provided by Advanced Research Computing, a division of Information and Technology Services at the University of Michigan, Ann Arbor.

- [1] P. J. Roberts and B. A. Jorns, Phys. Rev. Lett. **132**, 135301 (2024).
- [2] D. G. Brick and B. A. Jorns, IEPC 411, 38th international electric propulsion conference (2024).
- [3] P. J. Roberts et al, IEPC 393, 38th international electric propulsion conference (2024).
- [4] T. D. Arber et al, Front. Astron. Space Sci. 10:1155124 (2023).

Using AWSoM Simulations to Compare to Laboratory Experiments * <u>Khalil Bryant</u>, Matthew Trantham, Nishtha Sachdeva and Carolyn Kuranz University of Michigan (kalelb@umich.edu)

Interplanetary Coronal Mass Ejections (ICMEs) are solar eruptions that are the sources of geomagnetic storms which can cause severe damage to electrical systems and satellites. Research on them is typically from simulations and satellite observations, however, earlier this year we published an experimental paper on scaling of ICME events to be completed in the lab.[1] The paper compared the experimental results to satellite data, and doing so with simulation results provides further evidence of the veritability of the experiment.

* This work is funded by the US Department of Energy Office of Science Fusion Energy Sciences under award DE-SC0023336.

References

[1] Bryant, K., et al. "Creating and studying a scaled interplanetary coronal mass ejection." Physics of Plasmas **31**, no. 4, 1 Apr. 2024, https://doi.org/10.1063/5.0187219.

Extended Hydrogen Plasma Etching of (100) Single Crystal Diamond to Improve MPACVD Growth Quality

<u>Sarah P. Frechette Roberts</u> ^a, Alex J. Loomis ^a, Aaron Hardy ^b, Jonas N. Becker ^{a,b}, and Shannon S. Nicley ^{a,b}

(a) Quantum Optical Devices Laboratory, Michigan State University, East Lansing (rober964@msu.edu)

(b) Coatings and Diamond Technologies Division, Center Midwest (CMW), Fraunhofer USA Inc., East Lansing, MI

Substrate surface preparation is a crucial step for the growth of high-quality single crystal diamond (SCD) using chemical vapor deposition. The effects on the surface condition of a SCD substrate as a function of time of hydrogen etching was characterized to determine if an extended hydrogen etch removed damage detrimental to a diamond growth.

Two SCD substrates (NDT) were used in this study. The misorientation of NDT22 08b and NDT22_07 was 0.4° and 1.4° to the (100) surface, respectively. A hydrogen plasma at 320 mbar was used to etch the substrate. The hydrogen flow rate was 400 SCCM. The microwave power was adjusted to maintain a substrate temperature of 700°C. The substrate was incrementally etched for a total of 5 hours. The first etch series (NDT22_08b) contained several shorter increments whereas the second series contained fewer, longer etch steps. Each sample was then examined via differential interference contrast microscopy (DICM) to characterize the morphology. The surface roughness (Sa) of the substrates was measured by an averaging of three 10µm by 10µm scans using

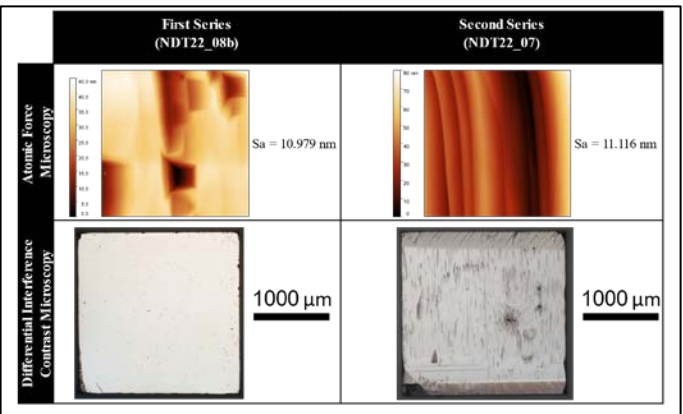


Figure 1 - AFM and DICM images of two samples after a 5-hour cumulative hydrogen etch. AFM results showing surface roughness and fine morphology and DICM images showing macro morphology.

atomic force microscopy (AFM) after each incremental etch. After a 5-hour hydrogen etch, the samples had similar Sa roughness but significantly different morphologies with NDT22_07 having substantially more etch pits with greater definition suggesting more damage was present on the original substrate.

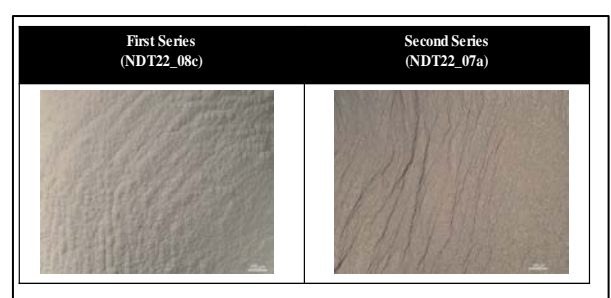


Figure 2 - DICM images showing growth morphology of NDT22_08c and NDT22_07a. Step flow growth is observed for both samples. A combination of step flow growth and orange peel growth is observed on NDT22 08c.

To conclude this study, the substrates in the post 5-hour hydrogen etch condition were used as the substrate for a chemical vapor deposition (CVD) diamond growth. Morphological analysis showed step flow growth, an indicator of good quality growth, on both substrates implying the extended hydrogen etch removed detrimental damage prior to deposition. By comparing the results of this investigation to other sample preparation methods such as reactive ion etching (RIE) and chemical mechanical polishing (CMP) our goal is to develop an optimized sample preparation method for the growth of high-quality single crystal diamond via CVD.

Channel Formation and Transverse Ion Acceleration from High-Intensity Laser Interactions with Underdense Plasma on OMEGA EP*

V. Contreras ^a, H. Tang ^{a,e}, F. Albert ^c, P. T. Campbell ^a, H. Chen ^c, Y. Ma ^a, P. M. Nilson ^d, B. K. Russell ^{a,f}, J. L. Shaw ^c, K. Tangtartharakul ^b, I-L. Yeh ^b, A. V. Arefiev ^b and L. Willingale^a

(a)University of Michigan (vacontre@umich.edu)
(b)University of California San Diego
(c) Lawrence Livermore National Laboratory
(d) Laboratory for Laser Energetics
(e) Lawrence Berkeley National Laboratory
(f) Princeton University

Experiments were performed at the OMEGA EP laser facility to study the direct laser acceleration (DLA) of electrons in an underdense plasma created from a helium gas target. In these experiments, the ponderomotive force expels electrons from the regions of highest laser intensity to form a channel. The charge separation creates a strong transverse electric field that accelerates ions radially through a Coulomb explosion; it is the same radial channel field, along with the electron beam-generated azimuthal magnetic field, that facilitates DLA. Since the channel formation is key to understanding electron acceleration, the transversely accelerated helium ions, measured with a Thomson Parabola Ion Energy (TPIE) spectrometer, provide an interesting complementary measurement for understanding the electric field strengths inside the channel. Furthermore, from data collected with a proton probe we aim to understand the properties of the channel fields, the same fields from which the ions have been accelerated.

*This work is supported by the Department of Energy / NNSA under Award Number DE-NA0004030 and DE-SC0021057. The experiment was conducted at the Omega Laser Facility at the University of Rochester's Laboratory for Laser Energetics with the beam time through the National Laser Users Facility (NLUF) program. The OSIRIS Consortium (UCLA and IST, Lisbon, Portugal) is acknowledged for providing access to the OSIRIS 4.0 framework. Work supported by NSF ACI-1339893.

Solar Wind Drivers of Auroral Omega Bands

Vivian Cribb, Tuija Pulkkinen and Connor DiMarco

University of Michigan Department of Climate and Space Sciences and Engineering (vcribb@umich.edu)

Space weather that occurs on Earth is a result of energy transfer from the sun to the Earth through the solar wind. When the solar wind magnetic field is oriented southward, the topology of the Earth's magnetic field changes through magnetic reconnection. This allows high energy particles from the solar wind to penetrate into the Earth's magnetosphere and precipitate into the upper atmosphere, where they excite neutral atoms. The photons released create the aurora borealis and australis in the northern and southern polar caps respectively.

Omega bands are a mesoscale auroral pattern that appear as eastward moving quasi-periodic protrusions in the auroral oval. These structures visually resemble the Greek letter omega, and may be used as a diagnostic for magnetic perturbations at Earth. They typically appear during magnetic storms and other periods of geomagnetic activity. However, their sources in the solar wind and the magnetosphere are not well understood [1].

In this work, we perform a statistical analysis of solar wind data from near-Earth satellites and ground magnetometer data taken during 28 omega band events from 2006 to 2013 to identify their solar wind drivers. We find local enhancements in the solar wind flow speed, magnetic field, pressure, and proton density at the time of the omega band observation. These features are consistent with geomagnetic activity associated with local compression regions in the solar wind.

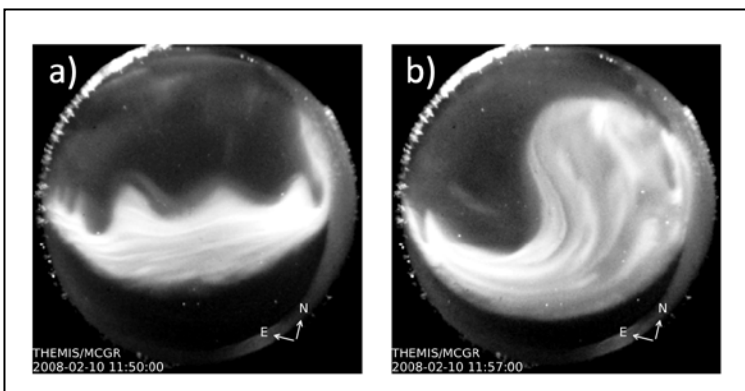


Figure 1 - Omega bands seen in an all sky imager camera located at McGrath.

Reference

[1] V. Cribb, T.I. Pulkkinen, L. Kepko, B. Gallardo-Lacourt, and E. Donovan, Geophys. Res. Lett. **51**, 109756 (2024).

High Energy Particle Measurements at Geostationary Orbit and their Relationship with Omega Band Formation

Connor DiMarco, Tuija Pulkkinen and Vivian Cribb

University of Michigan Department of Climate and Space Sciences and Engineering (cdimarco@umich.edu)

Earth's magnetic field and its interaction with the Sun form a complex system known as the magnetosphere. High energy particles that are ejected from the Sun can enter Earth's magnetosphere, particularly in the region "behind" the planet, known as the magnetotail. When these particles are injected into the tail, they are accelerated towards the Earth through a process called magnetic reconnection. These high energy particles can be observed in several ways, one of which being through satellite measurements.

Los Alamos National Laboratory (LANL) hosts multiple satellites at geostationary orbit, the region where the satellite revolves around the Earth at the same rotational speed as the planet, allowing the satellite to remain over one fixed point on the surface as it orbits. We use the Synchronous Orbit Particle Analyzer

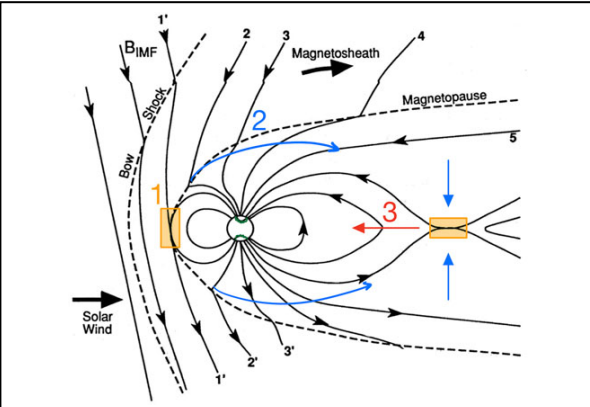
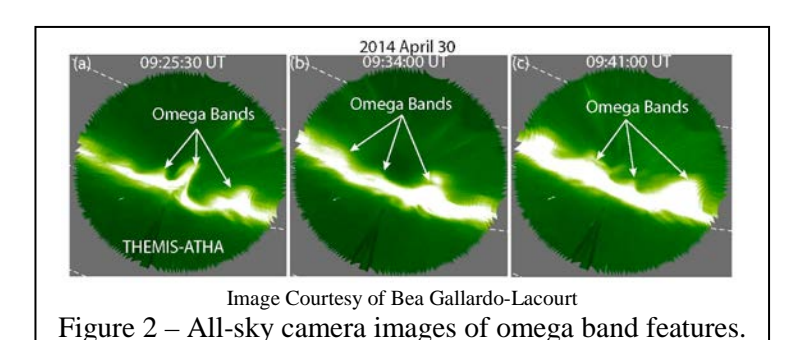


Figure 1 - A basic illustration of Earth's magnetosphere [1]. Plasma is injected into the tail region behind the Earth, and is accelerated towards the planet.

(SOPA) and Magnetospheric Plasma Analyzer (MPA) instruments on board these satellites to measure the particle fluxes at geostationary orbit.

Omega bands are structures in the aurora that typically appear during periods of enhanced activity in Earth's magnetosphere and resemble the Greek letter omega [2]. While omega bands are commonly seen during geomagnetic storms, their sources and the magnetospheric conditions in which they appear are not well understood. Omega bands have previously been mapped to regions between 5 and 13 RE in the magnetotail, indicating the importance of plasma sheet electrons to their formation. We use the LANL satellites to measure these plasma sheet electrons and determine their origin and evolution.



- [1] J. C. Foster et al., Front. Astron. Space Sci. 8, 786308 (2021).
- [2] V. Cribb et al., Geophys. Res. Lett. **51**, 109756 (2024).

Stability Analysis of Dynamic Screw-Pinch Driven Thin-Foil Liner Implosions *

A. Bedel, J. Chen, L. Tafoya, N. M. Jordan and R. D. McBride

University of Michigan, Ann Arbor (abedel@umich.edu)

Z-pinch implosions are susceptible to the fast-growing magneto-Raleigh-Taylor instability (MRTI) and to current-driven instabilities such as the m=0 "sausage" instability, the m=1 "kink" instability, and helical instabilities with m≥1 in general. In magnetized liner inertial fusion experiments (MagLIF), these instabilities reduce energy coupling to the target fuel and detrimentally impact fusion yield. One proposed MRTI mitigation technique is to use a dynamic screw-pinch (DSP) return current structure, which generates a helical magnetic field with a time-varying pitch angle to drive the implosion. The DSP has been shown to reduce MRTI growth, and recent numerical simulations indicate that MRTI mitigation increases with the initial ratio of axial magnetic field to azimuthal field (i.e. the initial drive field ratio). [1][2]

To experimentally investigate the effects and potential limits of MRTI mitigation in DSP implosions, a suite of return-current structures was designed and tested on the MAIZE linear transform driver at the University of Michigan. The suite allows a large range of initial drive field ratios to be tested (~0.3 to >1.0) while minimally impacting the load inductance of the system. This was accomplished using various pitch angles, radii, and number of intertwined helices in the return-current structures. The experiments were performed using 400-nm-thick metal foil liners. The implosion dynamics were captured using a 12-frame optical self-emission camera. Results from this study will be presented, along with considerations for future experiments.

* Work supported by NSF Grant PHY-2205608 and by the NNSA SSAP under DOE Cooperative Agreement DE-NA0004148.

- [1] P. Campbell et al. PRL 125, 035001 (2020)
- [2] G. A. Shipley et al. PoP 31, 022704 (2024)

Molecular Dynamics Simulations of Temperature Relaxation Rates for Strongly Magnetized, Ion-Electron, Antimatter Plasmas

James C. Welch III a, Louis Jose a, Tim D. Tharp b and Scott D. Baalrud a

(a) University of Michigan (welchjc@umich.edu)(b) Marquette University

Antimatter appears in minuscule quantities relative to matter in nature for reasons not yet fully understood. A better understanding of the fundamental physics governing antimatter is needed to aid in addressing this open question. The ALPHA experiment at CERN is working to improve our understanding of antimatter by trapping antihydrogen. The plasmas used to form the antihydrogen fall into the very strongly magnetized regime, meaning that the gyrofrequency exceeds the plasma frequency [1] and in the moderate Coulomb coupling regime denoting that the potential energy of interaction is on the order of the kinetic energy [2]. The traditional Coulomb collision frequency is modified in these regimes [3].

A recent theoretical study [4] has shown that the temperature relaxation process is an ion-electron plasma of arbitrary magnetization strength is described by 11 relaxation rates. Molecular dynamics (MD) simulations performed using the open-source software, LAMMPS [5] are used to benchmark the theory. A Nose-Hoover thermostat is used to bring the system to its equilibrium configuration. The velocities of each species are scaled such that a temperature difference is created. The simulation is switched to the NVE phase, and the magnetic field is turned on. The resulting temperature relaxation provides excellent agreement with the theory.

Here, we find reduced temperature relaxation models for the regime where electrons are strongly magnetized but ions are not. The temperature relaxation process in this regime can be described by only 2 rates using these reduced models. Using these reduced models, we find great agreement between the relaxation rates from MD and theory. This work validates recent theoretical findings on ion-electron temperature relaxation rates that may be studied in future antimatter plasma experiments in this novel, strongly magnetized regime.

* This material is based upon work supported by the U.S. National Science Foundation under Grant No. PHY-2205506. It used Expanse at San Diego Supercomputer Center through allocation PHY-150018 from the Advanced Cyberinfrastructure Coordination Ecosystem: Services & Support (ACCESS) program, which is supported by National Science Foundation grants #2138259, #2138286, #2138307, #2137603, and #2138296.

References

- [1] S. D. Baalrud and J. Daligault, "Transport regimes spanning magnetization-coupling phase space," Physical Review E **96**, no. 4, 2017.
- [2] G. B. Andresen et al, "Compression of antiproton clouds for antihydrogen trapping,"

Phys. Rev. Lett. 100, p. 203401, May 2008.

- [3] L. Jose and S. D. Baalrud, "A kinetic model of friction in strongly coupled strongly magnetized plasmas," Physics of Plasmas **28**, no. 7, 2021.
- [4] L. Jose and S. D. Baalrud, "Theory of the ion–electron temperature relaxation rate in strongly magnetized plasmas," Phys. Plasmas **30** (5), 052103 (2023).
- [5] Thompson A P et al 2022 LAMMPS—a flexible simulation tool for particle-based materials modeling at the atomic, meso and continuum scales Comput. Phys. Commun. 271 108171.

Generation of Ordered Atomic Gold Nanowires via Tip-enhanced Terahertz Field *

Sheng H. Lee a, Woei-Wu (Larry) Pai b and Tyler L. Cocker a

- (a) Department of Physics and Astronomy, Michigan State University (Leeshen1@msu.edu)
- (b) Center of Condensed Matter Sciences, National Taiwan University (wpai@ntu.edu.tw)

In terahertz scanning tunneling microscopy (THz-STM)¹⁻⁴, the field of a tip-coupled THz pulse coherently controls electron tunneling. The enhanced THz fields can apply over 10 V across the STM junction without damaging the tip⁵.

Previously, we observed nanowire formation on a clean Au(111) surface upon illumination by strong THz fields. Before illumination, the tip had crashed into a sample surface containing seven-atom-wide graphene nanoribbons (GNRs). THz-field emission of GNRs was thus proposed as a potential method to transfer GNRs between substrates.

Further investigation has revealed that the nanostructures formed under strong THz illumination are single-atom-wide gold nanowires and not GNRs. The nature of the gold nanowires is verified by scanning tunneling spectroscopy (STS), which reveals the dispersion of the 1D states. Along with the generation of nanowires, we observe a previously unknown surface (2x2) superlattice on Au(111). This pattern is overlaid on the herringbone reconstruction.

* This work was supported by the Office of Naval Research (MURI award N00014-21-2537; DURIP award N00014-21-1-2636; grant N00014-21-1-2682)

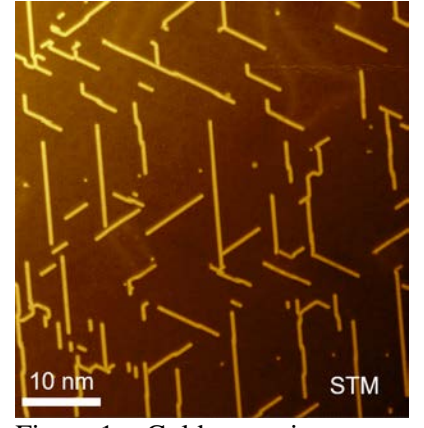


Figure 1 - Gold nanowires generated by the tip-enhanced THz field have a preferred growth direction along the close-packed directions. The longest nanowire generated in this way reach 35 - 40nm in length.

- [1] T. L. Cocker et al. "Nanoscale terahertz scanning probe microscopy," Nat. Photon. 15, 558 (2021).
- [2] T. L. Cocker et al. "An ultrafast terahertz scanning tunnelling microscope," Nat. Photon. 7, 620 (2013).
- [3] T. L. Cocker et al. "Tracking the ultrafast motion of a single molecule with femtosecond orbital imaging," Nature **539**, 263 (2016).
- [4] V. Jelic et al. "Ultrafast terahertz control of extreme tunnel currents through single atoms on a silicon surface," Nat. Phys. **13**, 591 (2017).
- [5] V. Jelic et al. "Atomic-scale terahertz time-domain spectroscopy," Nat. Photon. 18, 898 (2024).

Effect of Gas Temperature on the Chemical Vapor Deposition of Nanodiamond *

<u>Tanvi Nikhar</u> ^a, Sankhadeep Basu ^{b,c}, Shota Abe ^d, Shurik Yatom ^d, Yevgeny Raitses ^d, Rebecca

Anthony ^{b,c} and Sergey V Baryshev ^{a,b}

- (a) Department of Electrical and Computer Engineering, Michigan State University, East Lansing, MI (nikharta@msu.edu)
- (b) Department of Chemical Engineering and Material Science, Michigan State University, East Lansing, MI
 - (c) Department of Mechanical Engineering, Michigan State University, East Lansing, MI
 - (d) Discovery Plasma Science Department, Princeton Plasma Physics Laboratory, Princeton, NJ

Low-temperature plasmas have been used to develop hallmark processes in the microelectronics industry. Revolutionized by the discovery of size-dependent electronic properties in semiconductor nanocrystals, continuous flow-through reactors have been designed for nanoparticle synthesis with high production rates and simple means of sample collection. Well-vetted synthesis routes to produce semiconductor nanocrystals like diamond cubic Si, Ge, SiGe, etc. have been developed. However, diamond nanocrystals themselves have eluded these attempts.

In the present work, a capacitively coupled radio frequency (CCRF) plasma in a flow-through reactor design was first attempted to produce diamond nanoparticles (sp^3 phase carbon). However, synthesis of only graphitic nanoparticles (sp^2 phase carbon) was achieved. High-resolution optical emission spectroscopy (HR-OES) of the CCRF plasma revealed a maximum gas temperature of ~800 K. Since the kinetics involved in the formaton of diamond are slower and require a higher activation energy energy as compared to graphite, a higher gas temperature has been consistently reported in literature for diamond synthesis. To increase the power coupled to the plasma and ultimately the gas temperature, microwave plasma in the flow-through reactor assembly was tried instead. A gas temperature of ~2500 K was recorded using HR-OES and the resultant sample collected showed the presence of nanodiamond.[1]

A reactor-scale plasma model corresponding to the flow-through microwave reactor with H_2/CH_4 plasma chemistry is solved for the spatial distribution of C_xH_y (where x=1,2 and y=0-3) radicals. The electromagnetic absorption in the plasma and the corresponding gas heating and electron distribution functions are calculated. It is shown that the reactor is extremely efficient in producing atomic H and CH_3 radicals owing to the high gas temperature – all key parameters in producing sp^3 phase carbon.

* This work was supported by the U.S. Department of Energy, Office of Science, Office of Fusion Energy Sciences, Award No. DE-SC0023211, and National Science Foundation, Division of Chemical, Bioengineering, Environmental and Transport Systems, Award No. 2333452.

Reference

[1] T. Nikhar, S. Basu, S. Abe, S. Yatom, Y. Raitses, R. Anthony and S. V. Baryshev, J. Phys. D: Appl. Phys. **57** 475205 (2024).

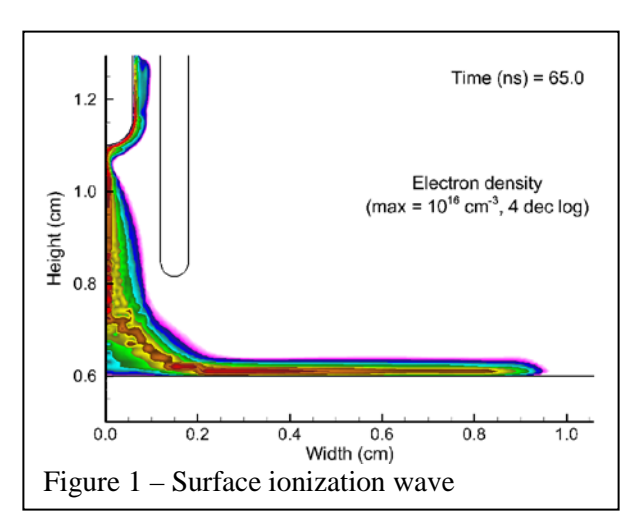
Dissociation Reaction Sources on Liquid Surfaces and PFAS Removal

Jisu Jeon, Mackenzie Meyer, Scott Doyle, Tiago C. Días and Mark J. Kushner

University of Michigan, Ann Arbor, MI (jisujeon@umich.edu)

When using negative discharges onto liquids at atmospheric pressure, an anode-like sheath forms at the liquid surface onto which electrons can be accelerated with energies of a few to tens of eV. When using positive discharges, analogous processes can occur with the formation of a cathode-like sheath accelerating positive ions into the liquid. Electrons striking the liquid surface can result in dissociation and ionization, which can be also induced by heavy particles and photons. These contributions to chemical activation of the liquid are poorly known [1] and can be a dominant mechanism in plasma-based water treatment intended to degrade surfactant-like molecules such as PFAS.

In this paper, the degradation of surface-resident molecules in liquids using atmospheric pressure plasma jet (APPJ) will be computationally investigated using *nonPDPSIM*, a 2-dimensional model in which multiphase plasmas can be addressed. The investigation aims to evaluate the contribution of electron, heavy particle, and photon impact dissociation on water surface compared to that of solvation and secondary reactions. The test systems are pulsed negative discharges onto the water and the surface ionization wave propagates along the surface as shown in Figure 1.



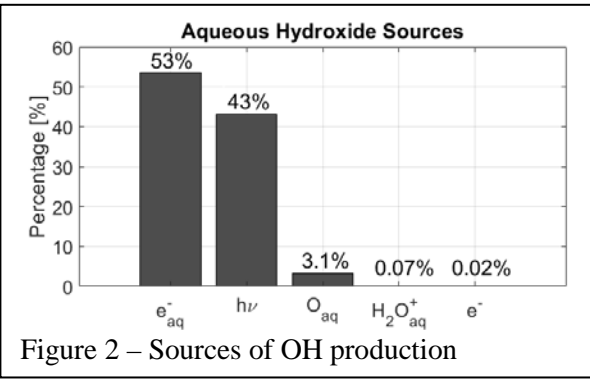


Figure 2 shows the sources of OH production in the water surface layer in this system. Photolysis accounted for 43%, while recombination between solvated electrons and water ion contributed to 53% of total production. The dissociation of fluorocarbon molecules residing on the water surface will be discussed as an example of dissociation on water with a surfactant.

* This work was supported by the US Department of Energy Office of Fusion Energy Sciences (DE-SC0020232), the Army Research Office MURI program (W911NF-20-1-0105), the National Science (CBET 2032604) and the 3M Company.

Reference

[1] P. J. Bruggeman et al, Plasma Sources Sci. Technol. 25, 053002 (2016).

Optimal Experimental Design for 2D Electron Measurements in a Hall Effect Thruster Channel

Madison G. Allen, Parker J. Roberts and Benjamin A. Jorns

University of Michigan (mgallen@umich.edu)

The electron dynamics of Hall Effect thrusters is a poorly understood concept due to the problem of anomalous transport. A Hall thruster is an annular in-space electric propulsion device that utilizes crossed electric and magnetic fields to generate a plasma and propel it from the thruster's channel. As electrons enter the channel from an electron source, they tend to cross magnetic field lines at a higher rate than can be explained by classical collisional theory. This additional flux is known as anomalous transport. Researchers have attempted to study this effect with probe techniques that have been proven to perturb the plasma in the near-field of the thruster. A novel diagnostic, Thomson scattering, has recently been applied to Hall thrusters and can directly measure electron properties without disrupting the plasma. This diagnostic measures the electron velocity distribution function from scattered light when a laser is introduced by employing the Doppler effect.

One challenge with this diagnostic is the noise in the signal. Thus, a large number of measurements are necessary to average over this noise for a clear signal. This process can take a few minutes for a single position. When exploring the electron properties in a 2D space, the experiment becomes expensive to perform. One solution to this cost problem is to limit the number of measurements and determine the positions in the 2D space where direct measurements are most informative. These measurements can be used to extrapolate to other regions of the space. By using the function Expected Information Gain, an optimal experimental design is determined with the positions that are most likely to accurately define the space of electron properties. In this work, the optimal 2D positions are determined via EIG applied to a low-fidelity electron mobility model. The experiment is then performed according to this result and the measured properties are extrapolated throughout the space. This work can be applied to directly calculating the cross-field mobility as a step towards a better understanding of electron dynamics in a Hall thruster.

* Work supported by a NASA Space Technology Graduate Research Opportunity and NASA Research Institute, JANUS.

- [1] Meezan, N. B., Hargus, W. A., and Cappelli, M. A., "Anomalous electron mobility in a coaxial Hall discharge plasma," Physical Review E **63**, 2001, p. 026410.
- [2] Jorns, B., Goebel, D. M., & Hofer, R. R., "Plasma Perturbations in High-Speed Probing of Hall Thruster Discharge Chambers: Quantification and Mitigation," 51st AIAA/SAE/ASEE Joint Propulsion Conference, American Institute of Aeronautics and Astronautics.
- [3] Vincent, B., Tsikata, S., and Mazouffre, S., "Incoherent Thomson scattering measurements of electron properties in a conventional and magnetically-shielded Hall thruster," Plasma Sources Science and Technology **29**, 2020, p. 035015.
- [4] Ryan, K. J., "Estimating Expected Information Gains for Experimental Designs With Application to the Random Fatigue-Limit Model," Journal of Computational and Graphical Statistics **12**, 2003, pp. 585–603. [5] Roberts, P. J., and Jorns, B. A., "Laser Measurement of Anomalous Electron Diffusion in a Crossed-Field Plasma," Physical Review Letters **132**, 2024, p. 135301.

Abstracts: Poster Session II

Experimental Investigation into the Role of Wall Materials in Electron Cyclotron Resonance Magnetic Nozzle Thrusters

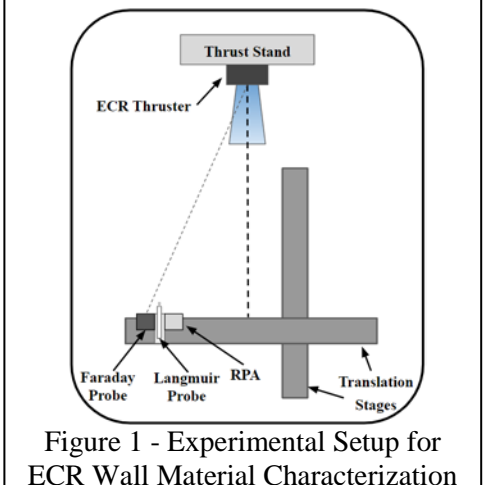
Ari Eckhaus and Benjamin Jorns

University of Michigan, Aerospace Engineering Department (aeckhaus@umich.edu)

Electron cyclotron resonance (ECR) thrusters are a promising low power electric propulsion (EP) technology. These devices use a highly efficient heating scheme to couple microwave power to the electrons of a plasma. The hot electrons are expanded through a diverging magnetic field, which, similar to a conventional rocket nozzle, serves to convert thermal energy into directed kinetic energy. This electron motion establishes an ambipolar field that accelerates ion downstream, generating thrust on the device. This principle of operation offers several key advantages for low power, small satellite applications. Specifically, ECR thrusters can operate without a hollow cathode, which is typically the life-limiting component in other EP devices. Furthermore, the ECR heating scheme has been experimentally shown to couple over 90% of the input microwave power to the plasma, allowing for efficient electron heating, even at low power inputs (<50 W). [1],[2] Despite these advantages, however, there are several fundamental questions that persist about the physics of ECR thrusters. In the effort to optimize performance of these devices, it is crucial to investigate these physical questions and characterize the loss mechanisms, to inform future thruster design considerations.

One open area of research surrounding ECR thruster operation concerns plasma interactions with the walls of the plasma source region. In principle, we expect the approximately axial magnetic field in the source to confine the plasma, limiting radial wall losses. However, it has previously been shown that global performance of the thruster (thrust and total efficiency) changes significantly when the radial wall material is changed.[3] This suggests there are indeed processes occurring at the radial wall that impact thruster behavior, but the underlying plasma physics have yet to be investigated experimentally.

In this work, we seek to quantify the differences in plasma behavior when the wall material within the ECR thruster source region is changed. Utilizing the test setup shown



ECR Wall Material Characterization

in Fig. 1, we will employ a suite of plasma diagnostics (Faraday probe, Retarding Potential Analyzer, and Langmuir probe) to measure the properties of the ECR thruster plume when operating with walls made of graphite, aluminum and boron nitride. From these measurements we will perform a breakdown of the efficiency modes of the thruster to determine physical reasoning for the previously observed changes to thruster performance.

- [1] B. Wachs, PhD Dissertation, University of Michigan (2022).
- [2] S. Peterschmitt, PhD Dissertation, Institut Polytechnique De Paris (2020).
- [3] T. Vialis et al., J. Propulsion and Power **34**, 5 (2018).

Space-Charge Induced Distortion of Short-Pulse Beams in a Vacuum Drift Space *

Yves Heri, Peng Zhang

Michigan State University, East Lansing, MI (heriyves@msu.edu)

The broadening of electron beams during their transport in a vacuum drift space is a critical challenge, particularly for applications requiring high spatial and temporal precision [1]. As the space-charge effect intensifies with increasing charge density or decreasing pulse length, the repulsive forces between electrons cause significant beam broadening, resulting in pulse length expansion as the beam propagates through a drift space. To quantitatively assess this broadening, we introduce a distortion metric, defined as the ratio of the final pulse length to the initial pulse length after a set propagation distance.

$$Distorsion = \frac{\Delta t_{sp}}{\tau_p}$$
 (1)

where Δt_{sp} is the temporal broadening due to space-charge effects, defined as the time difference between the front and trailing electrons reaching the downstream electrode, and τ_p is the initial pulse length. Using this definition, the beam distortion can be analytically derived [1]. For an injection energy eV_0 and drift space distance d, the single electron transit time is $T_0 = d/\left(\frac{2eV_0}{m_e}\right)^{1/2}$, where m_e is the electron mass. The space-charge-limited charge density in the drift space is $\rho_1 = -4\varepsilon_0 V_0/d$, where ε_0 is the permittivity of free space. We define the normalized initial pulse length as $k = \tau_p/T_0$ and normalized beam charge density $f = \rho/\rho_1$. With these normalized parameters, an analytical expression for the distortion

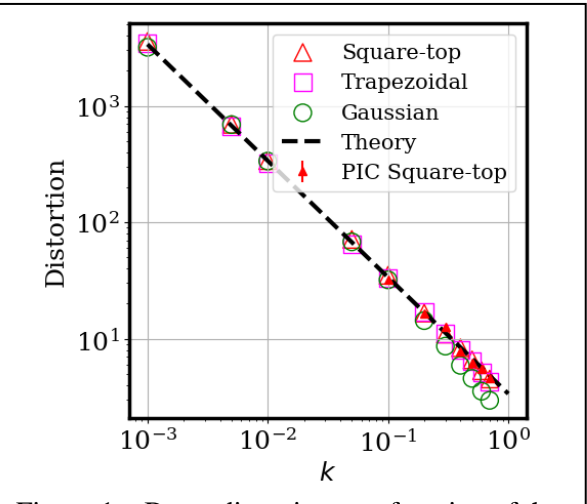


Figure 1 – Beam distortion as a function of the normalized pulse length k, for normalized charge density f = 1.

is obtained as Distorsion = 27f/8k. Using the multiple-sheets model for various beam profiles and XOOPIC simulations with a drift space distance d = 1 cm and injection energy $eV_0 = 1$ keV, Figure 1 illustrates the beam distortion as a function of the normalized pulse length k, for a normalized charge density f = 1. By correlating this metric with charge density, pulse duration, and beam energy, we aim to characterize the extent of distortion and identify the thresholds where the space-charge forces lead to significant degradation in beam quality.

* Work is supported by the Office of Naval Research (ONR) YIP Grant No. N00014-20-1-2681, the Air Force Office of Scientific Research (AFOSR) Grant No. FA9550-20-1-0409, and the Air Force Office of Scientific Research (AFOSR) Award No. FA9550-22-1-0523.

- [1] Bao-Liang Qian, Hani E. Elsayed-Ali, J. Appl. Phys. **91** (1): 462–468 (2002).
- [2] P. Zhang, W. S. Koh, L. K. Ang, S. H. Chen, Phys. Plasmas 15 (6): 063105 (2008).

Hydrogen Sensor via Plasma Techniques Development *

Sarah Feldman ^a, Kenneth Engeling ^b, Carolina Franco ^b, Nicholas Spangler ^c and Jessica Schwend ^b

(a) University of Michigan (sarfeldm@umich.edu)

(b) NASA Kennedy Space Center Applied Chemistry Laboratory

(kenneth.engeling@nasa.gov, carolina.franco@nasa.gov, jessica.schwend@nasa.gov)

(c) NASA Kennedy Space Center Applied Physics Laboratory (nicholas.b.spangler@nasa.gov)

Currently, NASA Kennedy Space Center's Exploration Ground Systems (EGS) uses liquid hydrogen (LH₂) as fuel for launches and ensures hydrogen is no longer in the fill lines by sampling gas into a controlled environment. Then they use a catalytic sensor that detects when hydrogen interacts with

oxygen. However, this procedure requires repeatedly backfilling and flushing with helium, which can be wasteful during a global helium shortage and expensive for each sampling port. Therefore, the team at KSC set out to establish proof-of-concept of a plasma-based hydrogen sensor that is anaerobic – and can in fact detect in most environments and below atmospheric pressures – and with a small footprint and more sensitive than other hydrogen sensors currently on the market.

The technology development was done by testing known concentrations of hydrogen in argon gas fed through a vacuum cube

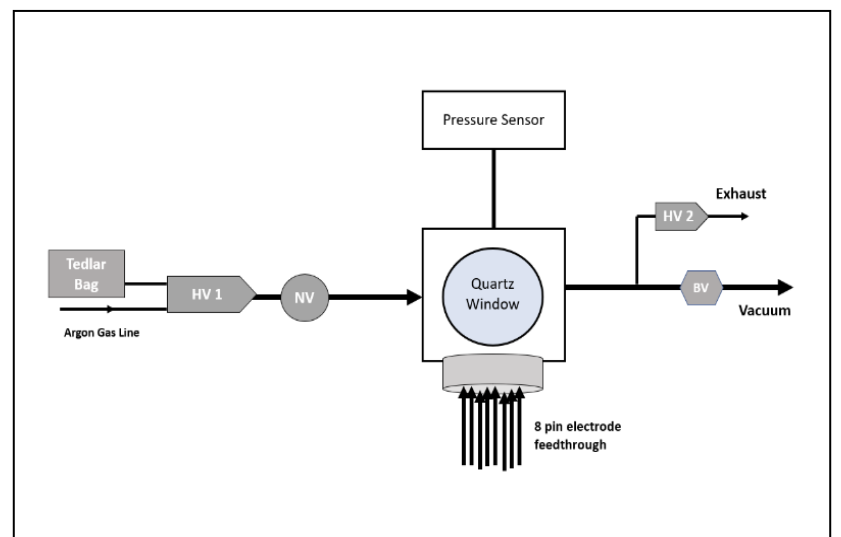


Figure 1 - Simple schematic of the plasma-based hydrogen sensor setup (not to scale).

containing an electrode feedthrough at varying pressures. The resultant emission spectra were recorded with a fiber optic spectrometer and analyzed to determine the instrument's accuracy. Throughout testing, efforts were made to prove the off-the-shelf capabilities of the setup. The traditional high voltage AC-power source was switched to an affordable, handheld plasma lighter. Additionally, the spectrometer was supplemented with a double photodiode circuit to take targeted measurements of the Balmer- α and - β lines in the hydrogen spectrum.

From this, we established a proof of concept sensor. SLS required it to detect as low as 100 ppm whereas we detected hydrogen in concentrations as low as 50 ppm and in an anaerobic environment.

* Work supported by NASA Kennedy Space Center's Science Mission Directorate Innovative Research and Development Fund.

Onset of Silicon Nanoparticle Crystallinity in Nonthermal Plasmas *

Yifan Gui ^a and Mark J. Kushner ^b

- (a) Department of Nuclear Engineering and Radiological Sciences (evangyf@umich.edu)
- (b) Department of Electrical Engineering and Computer Science (mjkush@umich.edu) University of Michigan, Ann Arbor, MI

Group IV nanoparticles (NPs) have a wide range of applications in the semiconductor, catalyst and biomedicine fields due to their favorable electrical and optical properties. Nonthermal plasma synthesis is an attractive method to control NP size uniformity and produce crystalline NPs that contain minimal charge carrier traps and defects. Prior experimental and computational work [1] propose that the crystallinity of NPs synthesized in plasmas are likely the result of stochastic particle heating by surface reactions.

This paper discusses results from computational investigations of heating and crystallization of NPs in inductively coupled plasmas (ICPs), capacitively coupled plasmas (CCPs) and pulsed plasmas. The Hybrid Plasma Equipment Model (HPEM) coupled with Dust Transport Simulator (DTS) allows for the temporal and spatial tracking of NP properties in nonthermal plasmas. The DTS has been improved to track the temperature of individual nanoparticles through ion and neutral particle interactions. The test system is a cylindrical CCP with a single plasma source that operates at a pressure of a few Torr, 10 W of CCP power and with Ar/SiH₄ as the feed gas. The impact on the temperature-dependent crystallization of Si NPs of an expanded operational space (plasma type, power, pressure, mixture) and mechanisms of crystallization will be discussed.

* Work supported by Army Research Office (W911NF-18-1-0240) and the Department of Energy Office of Fusion Energy Science (DE-SC0020232, DE-SC0024545).

Reference

[1] Kramer et al, J. Phys. D: Appl. Phys. 47, 075202 (2014).

Two-Frequency RF Fields Induced Multipactor in Coaxial Transmission Line *

Md Mashrafi ^a, Asif Iqbal ^a, John Verboncoeur ^{a,b}, and Peng Zhang ^a

- (a) Department of Electrical and Computer Engineering, Michigan State University, East Lansing, Michigan
- (b) Department of Computational Mathematics, Science, and Engineering, Michigan State University, East Lansing, Michigan

(mashrafi@egr.msu.edu, iqbalas3@egr.msu.edu, johnv@egr.msu.edu, pz@egr.msu.edu)

This work investigates multipactor discharge in coaxial geometry [1] with two-frequency rf electric field

 $V_{rf}[\sin(\omega t + \theta) + \beta \sin(n(\omega t + \theta) + \gamma)],$ where V_{rf} is the peak voltage, β is the field strength of the second carrier mode relative to fundamental mode, n is the ratio of two carrier frequencies and γ is the relative phase of second carrier mode. We find that multipactor susceptibility depends strongly on β and γ , using Monte Carlo simulations [2,3]. Our calculation includes the effects of image charge. For various combination of twofrequency rf operation, in general, multipactor susceptibility band shrinks in comparison single-frequency operation (Fig. 1). Mixed Multipactor modes, consisting of single-surface impacts as well as two-surface impacts observed under two-frequency operation for certain gap distances and frequencies. Our multipactor susceptibility chart for single frequency perfectly matches with Woo's results[4]. As we increase the phase from $\gamma = 0$ to $\gamma = \frac{\pi}{2}$ the susceptibility chart shrinks.

* Work supported by AFOSR MURI Grant No. FA9550-18-1-0062 and FA9550-21-1-0367.

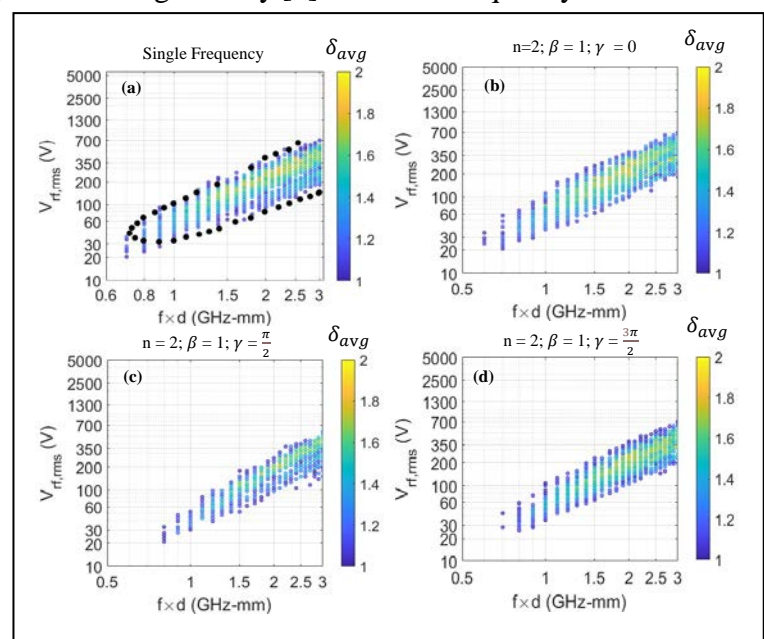


Figure 1 – Multipactor susceptibility charts in the $V_{rf,rms}$ – fd space calculated from Monte Carlo (MC) simulations with image-charge effects for (a) single frequency rf operation, (b)-(d) two-frequency rf operations with relative phase of the second carrier (b) $\gamma = 0$, (c) $\gamma = \pi/2$, and (d) $\gamma = 3\pi/4$, for fixed relative strength of the second carrier $\beta = 1$ and frequency ratio between the two carrier modes n = 2. Here, $V_{rf,rms} = V_{rf}/\sqrt{2}$ is the rms voltage of rf fields, f is the fundamental frequency and d is the gap distance. δ_{avg} is the average value of the secondary electron yield over 50 impacts in the coaxial line.

- [1] J. R. M. Vaughan, IEEE Trans. Electron Devices 35, no. 7, pp. 1172–1180 (1988).
- [2] A. Iqbal, Ph.D. Thesis, Michigan State University, Michigan, United States (2021).
- [3] A. Iqbal, J. Verboncoeur, and P. Zhang, Phys. Plasmas 25, 043501 (2018).
- [4] R. Woo, J. Appl. Phys. **39**, no. 3, pp. 1528–1533 (1968).

Development of an "Ion Mode" for SERENA/Strofio, the Low-Energy Neutral Particle Detector onboard BepiColombo *

Michael Hackett ^a, Stefano Livi ^{a, b} and Jim Raines ^a

(a) University of Michigan, Department of Climate and Space Sciences and Engineering (mthacket@umich.edu, slivi@umich.edu, jraines@umich.edu)
(b) Southwest Research Institute (SwRI) (stefano.livi@swri.org)

The BepiColombo spacecraft is currently en route to a November 2026 orbital insertion for science operations at Mercury, and consists of two orbiters: MPO (the Mercury Planetary Orbiter) and Mio (formerly "MMO", the Mercury Magnetospheric Orbiter). [1] Aboard MPO is SERENA (Search for Exospheric Refilling and Emitted Natural Abundances): an instrument suite of four independently-operated detectors designed to tackle core scientific objectives of the BepiColombo mission, particularly with respect to Mercury's evolutionary history and the planet's dynamic relationship with the Sun and the solar wind. SERENA is designed to observe a wide range of energies of both ions and neutrals over its four detectors, with unique guiding objectives for each. Tasked with measuring the lowest energy neutral particle composition and density, in the range of ~0 to a few eV, is Strofio. [2]

Strofio is a time-of-flight (TOF) neutral mass spectrometer that employs a novel rotating electric field technique to determine particles' TOF. This novel technique "stamps" particles with a TOF start-time as their resulting position on an annular detecting MCP is determined by the pointing direction of a rotating electric field at the time that the particle enters the detecting region. This design achieves a mass resolution of ≥ 84 m/ Δ m with a high sensitivity of 0.14 (counts/s)(particles/cm³), and a mass of only 4kg. [3]

MESSENGER (MErcury Surface, Space ENvironment, GEochemistry and Ranging) is the only previous orbital mission sent to Mercury, which orbited from 2011-2015, and carried the Fast Imaging Plasma Spectrometer (FIPS), a TOF mass spectrometer that measured the energy, angular, and compositional distributions of low-energy ions, from ~50 eV/charge to 20 keV/charge. [4]

By developing an ion mode for Strofio, the lowest-energy ions of Mercury's near-planet environment may be studied, particularly ~ 0 to ≥ 50 ev/charge, below FIPS' energy range. The most prominent sources of ionization in Mercury's exosphere produce ions in this range, particularly photoionization, electron-stimulated desorption, and sputtering, allowing for study of these ions before they are accelerated from the system. [6] This range also includes ions created via charge exchange of neutral exospheric atoms, allowing further study of the connection between the neutral exosphere and plasma environment. [5]

* Work supported by the National Aeronautics and Space Administration (NASA)

- [1] J. Benkhoff, G. Murakami, W. Baumjohann, et al. Space Sci. Rev. 217, 90 (2021).
- [2] S. Orsini, S. Livi, S. Lichtenegger, et al. Space Sci Rev. 271, 11 (2021).
- [3] R. Gurnee, S. Livi, M. Phillips, et al. IEEE Aero. Con. 1-11 (2012).
- [4] G. Andrews, T. Zurbuchen, B. Mauk, et al. Space Sci. Rev. 131 (2007).
- [5] D. Domingue, C. Chapman, R. Killen, et al. Space Sci. Rev. 181 (2014).
- [6] A. Mura, S. Orsini, A. Milillo, et al. Planetary and Space Sci. 54, 2 (2006).

Carbon Backsputter Mitigation with a Retarding Beam Dump *

<u>Braden Oh</u>, William Hurley, Grace Zoppi, Christopher May, Collin Whittaker and Benjamin Jorns

University of Michigan, Plasmadynamics & Electric Propulsion Laboratory (bradenoh@umich.edu)

The problem of backsputter, in which facility material sputtered by an ion beam returns to coat the source, impedes flight qualification testing of long lifetime electric propulsion thrusters by obscuring the erosion rate of critical components. This study demonstrates how electrostatic deceleration of Hall thruster beam ions prior to striking a beam dump may be used to reduce backsputter rates. A 'beam catcher' comprised of a positively biased graphite plate with a transverse magnetic field is tested. The magnetic

field enables high decelerating potentials to be applied to the beam dump while minimally affecting thruster performance. A 1.3×0.66 m prototype of this device was tested in the far-field plume of a 4.5 kW Hall effect thruster from biases of 0 V to 200 V and maximum magnetic field strengths from 0 G to 200 G. Measurements were made of the net backsputter rate at the thruster plane and of thruster operating metrics including the beam potential and shape of the far-field plume, the thrust, and the anode current oscillation spectrum. It was shown that the far-field plume potential and thrust levels do not vary within uncertainty at biases



Figure 1 – Photograph of the beam catcher (left) operating in the presence of a H9 Hall effect thruster beam (right).

up to 150 V and that anode current oscillation power spectrum maxima occur at identical frequencies. Plume divergence appears to increase with applied bias potential. Backsputter rates are found to vary from

 $2.91~\mu m/kHr$ for an unbiased beam dump to -1.99 $\mu m/kHr$ for a 150 V biased plate. The negative backsputter rates indicate an erosion process believed to be caused by ions generated via charge exchange near the plate being launched back at the thruster by the beam dump bias. The implications of these findings and strategies for mitigating ion backstreaming are discussed in the context of establishing novel boundary conditions for next-generation propulsion system testing.

* This work was supported by the Joint Advanced Propulsion Institute (JANUS), a NASA Space Technology Research Institute, and by the National Science Foundation Graduate Research Fellowship Program.

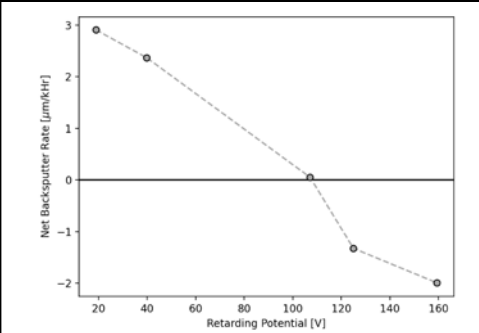


Figure 2 – Net backsputter rate as a function of ion retarding potential.

- [1] B. Oh et al, 38th International Electric Propulsion Conference, 504 (2024).
- [2] W. Hurley et al., AIAA SciTech Forum (2024).
- [3] S. Thompson et al., AIAA SciTech Forum (2024).

Optimization of Substitutional Phosphorus in n-type Diamond

Milos Sretenovic ^{a,b}, Sarah P. Frechette Roberts ^d, Alex J. Loomis ^{a,b}, Luke Suter ^c, Aaron Hardy ^c, Matthias Muehle ^c, Timothy P. Hogan ^a, Jonas N. Becker ^{b,c}, and Shannon S. Nicley ^{a,c,d}

- (a) Department of Electrical and Computer Engineering, Michigan State University, East Lansing, MI (sretenov@msu.edu)
 - (b) Department of Physics, Michigan State University, East Lansing, MI
- (c) Coatings and Diamond Technologies Division, Center Midwest (CMW), Fraunhofer USA Inc., 1449 Engineering Research Ct., East Lansing, MI
- (d) Department of Chemical Engineering and Materials Science, Michigan State University, East Lansing, MI

n-type diamond holds great potential for a wide array of technological applications, including quantum computing and sensing. Phosphorus is currently the most promising *n*-type dopant and has high potential for quantum devices. For example, long spin-coherence times in phosphorus-doped diamond has led to increased sensitivities of nitrogen-vacancy (NV) sensors, improved quantum fidelity, and longer quantum-memory times [1]. In addition, its inclusion in *p-i-n* junctions has been used to create single-photon sources which have applications in quantum communication, computing, and metrology [2]. Yet major challenges still exist such as phosphorus's low incorporation rate and a tendency to form phosphorus-vacancy complexes that compensate substitutional phosphorus atoms and reduce overall conductivity [3]. Achieving controllable levels of P is an area of significant interest [4-6] and so controlled parameter studies of the growth of P-doped diamond are needed.

To observe the substitutional behavior of phosphorus-doped diamond, we plan to grow two series of single-crystal P-doped diamond samples, one isothermal series and another isobaric series by Microwave-Plasma Assisted Chemical Vapor Deposition (MPACVD) using phosphine feed gas on (111) oriented single-crystal diamond substrates. The diamond reactor to be used excites microwaves within a resonant cavity to strike a plasma that sustains the chemical reaction needed for diamond growth. Our eventual goal will be to determine the optimized growth conditions for substitutional phosphorus and n-type conductivity.

- [1] N. Mizuochi, "Control of Spin Coherence and Quantum Sensing in Diamond" Springer (2021).
- [2] N. Mizuochi, et al., Nat. Photonics. **6**, 299 (2012).
- [3] R. Jones, et al., Appl. Phys. Lett. **69**, 2489 (1996).
- [4] R. Ohtani, et al., Appl. Phys. Lett. **105**, 232106 (2014).
- [5] H. Kato, et al., Appl. Phys. Lett. **109**, 142102 (2016).
- [6] T. A. Grotjohn, et al., Diamond Relat. Mater. 44, 129 (2014).

Effect of Secondary Electron Emission on Surface Charging during Plasma Etching for Microelectronics Fabrication *

Chenyao Huang a, Steven C. Shannon b and Mark J. Kushner a

(a) University of Michigan, Ann Arbor, MI(chenyaoh@umich.edu, mjkush@umich.edu)(b) North Carolina State University, Raleigh, NC(scshanno@ncsu.edu)

Plasma etching is a critical process in semiconductor device manufacturing. During this process ions having a broad range of energy and a narrow angular distribution are incident onto the wafer. Depending on the power format, electrons are incident onto the wafer with broad angle, low energy distributions or moderately energetic, moderately narrow distributions. These different energy and angular distributions lead to differential charging of the features being etched, which can in turn lead to feature distortion due to deflection of the trajectories of incoming particles. A phenomenon that is important in this process is secondary electron emission induced by ions, electrons and photons striking the surface. With secondary emission by electrons and ions being dependent on energy and angle, secondary electron emission can result in additional positive charging at the location of intial collision even by electrons. The secondary electrons are accelerated by the local electric field can deposit charge in a different location.

The Monte Carlo Feature Profile Model (MCFPM), a 3-dimensional voxel-based model, describes the physics and chemistry of feature schale etching and charge deposition. The MCFPM receives energy and angle resolved fluxes from the Hybrid Plasma Equipment Model (HPEM). The MCFPM capabilities for describing the emission of secondary electrons by ions, electrons, high-energy electron beam and photons have been improved. Charging of test structures in capacitively coupled plasmas sustained in argon with continous and pulsed excitation and the role of secondary emission will be discussed.

^{*} This work was supported by the Department of Energy Office of Fusion Energy Sciences (DE-SC0024545).

Radiation Hydrodynamics Simulations of the Photoionized Plasmas in Accretion-powered Objects Experiment on Z *

<u>Isaac Huegel</u> ^a, Patricia Cho ^b, Roberto Mancini ^c, Heath LeFevre ^a,

Matthew Trantham ^a, Guillaume Loisel ^d and Carolyn Kuranz ^a

- (a) University of Michigan (idhuegel@umich.edu)
 - (b) Lawrence Livermore National Laboratory
 - (c) University of Nevada Reno
 - (d) Sandia National Laboratories

Accreting black holes in X-ray binaries and active galactic nuclei constitute some of the most luminous objects in the universe. Model fits to reflection spectra from such systems have predicted unreasonably high Fe abundances, inconsistent with stellar evolutionary theory. This has revealed a need for increased scrutiny of the models. The Z machine at Sandia National Labs has a unique capability to probe the relevant physics. On the photoionized expanding foil platform, X-ray radiation from the Z-pinch is incident on a foil target, which reaches temperature, density, and photoionization conditions found in black hole accretion disks. It provides a means to benchmark astrophysical photoionized plasma codes (such as XSTAR) by measuring high resolution absorption and emission spectra, which can be used to test the underlying atomic physics in the models. We present initial results of simulations performed with the 1-D radiation hydrodynamics code HELIOS-CR to address questions of density and temperature gradients, evolving charge state distributions, and plasma expansion in the foil. Results from these simulations will help validate assumptions made in the spectroscopic analysis of data and facilitate more effective data-model comparisons.

* This work is supported by Sandia National Laboratories, a multimission laboratory managed and operated by NTESS LLC, a wholly owned subsidiary of Honeywell International Inc. for the U.S. DOE's NNSA under contract DE-NA0003525.

This work is funded by the U.S. Department of Energy NNSA Center of Excellence under cooperative agreement number DE-NA0003869.

P.B.C. acknowledges support from the DOE NNSA LRGF under U.S. Department of Energy cooperative agreement number DE-NA0003960.

P.B.C. acknowledges support from the Wootton Center for Astrophysical Plasma Properties under U.S. Department of Energy cooperative agreement number DE-NA0003843.

- [1] MacFarlane et al. HELIOS-CR A 1-D radiation-magnetohydrodynamics code with inline atomic kinetics modeling, Journal of Quantitative Spectroscopy and Radiative Transfer (2005).
- [2] Mancini et al. X-ray heating and electron temperature of laboratory photoionized plasmas, Physical Review E (2020).
- [3] Loisel et al. Benchmark Experiment for Photoionized Plasma Emission from Accretion-Powered X-Ray Sources, PRL (2017).
- [4] Garcia et al. The effects of high density on the X-ray spectrum reflected from accretion discs around black holes, MNRAS (2016).

Synthesis of Carbon Nanoparticles via RF Plasma Jet in the Atmosphere

Xitong Xu, Sankhadeep Basu and Rebecca Anthony

Michigan State University (xuxitong@msu.edu)

Sustainable conversion of fossil fuels such as methane (CH4) into added-value carbon products such as carbon nanostructures, including graphite or graphene nanoparticles, remains an important piece of the renewable energy transition. Flow-through plasma reactors are electricity-driven, versatile, and have the potential to be scalable integrated with other advanced manufacturing strategies. Previously we have demonstrated carbon nanoparticle formation from methane using a low-pressure RF plasma reactor, but transitioning this process to atmospheric pressure while maintaining the desirable properties of the carbon nanoparticles would further improve the integration of these plasma reactors into the manufacturing stream.

Here, we demonstrate synthesis of carbon nanoparticles via methane conversion using a radio-frequency (RF) plasma jet at atmospheric pressure. The plasma jet was generated from a mixture of precursor methane and carrier argon gases, pre-mixed prior to plasma formation. The resulting carbon nanoparticles were deposited onto a glass or copper substrate for analysis. In this study, we varied the flow rates of methane (1-5sccm) and argon (100-500sccm) while maintaining a discharge power of 100W to generate the RF plasma. X-ray diffraction (XRD) and Fourier-transform infrared spectroscopy (FTIR) were employed to examine the effects of different conditions on the crystallinity and surfaces of the nanoparticles. Additionally, Raman spectroscopy and transmission electron microscopy (TEM) were used to observe the characteristics of the deposited nanomaterials. Optical emission spectroscopy (OES) was applied to used to monitor the excited gas species and gas temperatures during the synthesis process. The results of this work will lead to a strengthened understanding of methane up-conversion into nanoparticles, using manufacturing-compatible plasma reactors.

Mass Utilization Scaling with Propellant Type of a Magnetically Shielded Hall Thruster William Hurley and Benjamin Jorns

University of Michigan (wjhurley@umich.edu)

Hall thrusters are now the most widely flown type of electric propulsion device. These devices employ perpendicular electric and magnetic fields to ionize and accelerate a plasma to high speeds for thrust generation. Therefore, ionizing a large fraction of the input propellant is key to efficient device operation. The majority of Hall thrusters to date have been optimized for high performance on xenon gas. Xenon is an attractive propellant option because it is easy to ionize, stores densely, and has a large atomic mass. However, xenon is an extremely rare gas in the Earth's atmosphere, making it expensive and subject to large price fluctuations. [1-2] Therefore, alternative, more available gases like krypton, argon, or even

nitrogen are being considered as a substitute. One challenge with using these alternative propellants is that they have smaller ionization cross sections and faster thermal velocities than xenon, making them harder to ionize. Therefore, the overall device efficiency is typically lower when operating on these gasses when compared to xenon. [3] In this work, we formulate a simple 0D scaling law to predict the Hall thruster ionization fraction for a given gas type and operating condition. This scaling law relates the global properties of the thruster discharge (voltage, current), and propellant (ionization cross section) to an equivalent ionization mean free path λ_i . We utilize a far field probe suite to gather experimental mass utilization data on each propellant for model validation. The results indicate that with a single learned parameter for the entire data set, the model accurately captures the

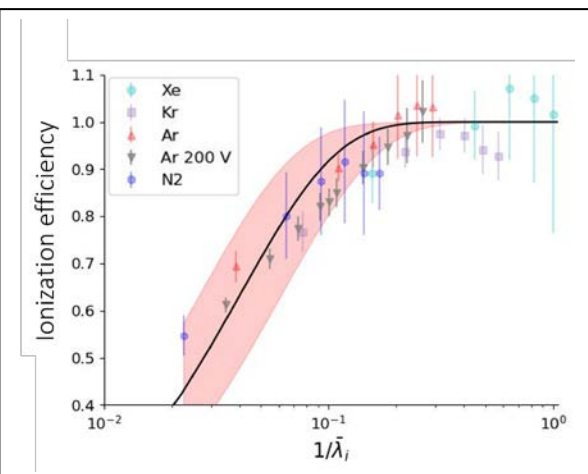


Figure 1 – Experimental data and mass utilization model plotted as a function of inverse ionization mean free path.

experimental data to within measurement uncertainty. We show a comparison of the model predictions to experimental data in Fig. 1. The agreement between our simple model and the experimental data indicates that we are accurately representing some of the underlying physics driving mass utilization. This physics-based understanding could be key for designing the next generation of Hall thrusters to operate efficiently on alternative propellants.

- [1] Well, R. "Availability considerations in the selection of inert propellants for ion engines." 21st International Electric Propulsion Conference (1990).
- [2] Herman, D. A., and Unifried, K. G. "Xenon acquisition strategies for high-power electric propulsion nasa missions." JANNAF SPS Subcommittee Meeting. No. GRC-E-DAA-TN23198 (2015).
- [3] Su, L. L., and B. A. Jorns. "Performance comparison of a 9-kW magnetically shielded Hall thruster operating on xenon and krypton." Journal of Applied Physics **130**.16 (2021).

Influence of Temporal Shapes of Femtosecond Laser Pulses on Photoemission from a Metal Surface *

Lan Jin and Peng Zhang

Department of Electrical and Computer Engineering, Michigan State University, East Lansing, Michigan (pz@egr.msu.edu)

In recent years, photoemission from metallic nanoparticles induced by ultrafast laser fields, typically in the femtosecond (10⁻¹⁵ seconds) range, has been intensively studied both theoretically and experimentally. It has a wide range of potential applications, including time-resolved photoemission electron microscopy, diffraction, high frequency electromagnetic radiation generation, and high-speed nanoscale vacuum devices. Besides laser intensity, the interaction between solid-state nanostructures and femtosecond laser pulses is also impacted by pulse profile, pulse length and phase, all of which play a

crucial role in governing the behavior of free and bound electrons. By utilizing femtosecond laser pulses induced photoemission, researchers can directly observe and manipulate electron dynamics in real-time, making this technique a powerful tool in the study of diverse fields, such as condensed matter physics, materials science, chemistry, and nanotechnology [1].

In this work, we investigate photoemission from an Au surface subjected to a weak DC field and a femtosecond laser pulse using an exact quantum model for photo- and field-emission processes [2-3]. We explore various femtosecond laser pulse shapes, including Gaussian (m=1 in Fig. 1), super-Gaussian (of different orders m=3, 5, and 10 in Fig. 1), hyperbolic secant squared (sech²), and \cos^2 profiles. Since different temporal shapes and pulse lengths (τ_p) modify the laser pulse spectrum, they are expected to influence electron dynamics in laser-matter interactions [4], as shown in Figure 1. The transmission probabilities for short pulse lengths (ranging from 0.5 to 10 fs) in the near infrared (800 nm) with these temporal profiles have been calculated.

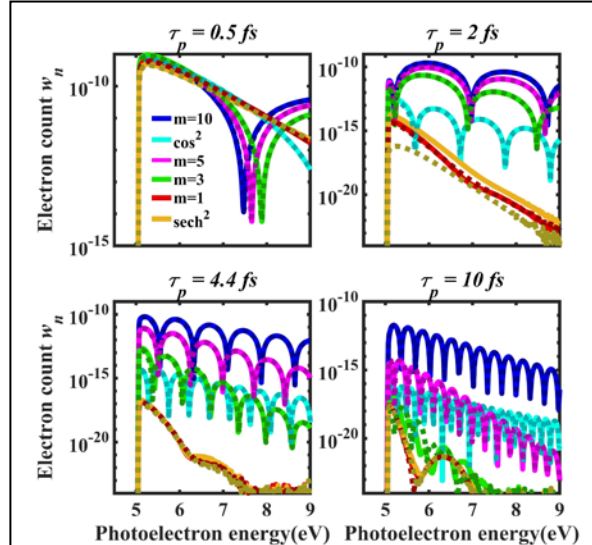


Figure 1 - Emission spectra per pulse w_n for various femtosecond pulse profiles with durations of 0.5 fs, 2 fs, 4.4 fs, and 10 fs, at a carrier-envelope phase of $\phi = 0$ (solid line) and $\phi = \pi$ (dotted line).

* Work supported by ONR YIP Grant No. N00014-20-1-2681, AFOSR Grant Nos. FA9550-20-1-0409 and FA9550-22-1-0523, and NSF Grant No. 2407060.

- [1] Dombi P, Pápa Z, Vogelsang J, et al. Rev. Mod. Phys. 92, 025003 (2020).
- [2] P. Zhang, and Y.Y. Lau, Sci. Rep. **6**(1), 19894 (2016).
- [3] Y. Luo, Y. Zhou, and Peng Zhang, Phys. Rev. B **103**, 085410 (2021).
- [4] Jouin H, Duchateau G, Phys. Rev. A 99, 013433 (2019).

Effects of Pulse Chirp on the Stability and Efficiency of Plasma Wakefield Photon Acceleration

Neil Beri a, Qian Qian b, Kyle Miller c, John Palastro c, and Alexander Thomas a, b

- (a) Department of Nuclear Engineering and Radiological Sciences, University of Michigan, Ann Arbor, MI (nebe@umich.edu, agrt@umich.edu)
 - (b) Department of Electrical and Computer Engineering, University of Michigan, Ann Arbor, MI (qqbruce@umich.edu)
 - (c) Laboratory for Laser Energetics, University of Rochester, Rochester, NY (kmill@lle.rochester.edu, jpal@lle.rochester.edu)

Ultrashort, coherent extreme ultraviolet (XUV) radiation sources are desired for their ability to probe nanoscale structures and ultrafast dynamics of physical systems. One method of producing XUV laser pulses is plasma wakefield photon acceleration (PWPA). When a relativistic electron beam injected into a plasma drives a nonlinear wakefield with large plasma density gradients, a witness laser in the downward gradient of the wakefield can be accelerated and frequency up-shifted. Particle-in-cell (PIC) simulations are performed using OSIRIS to analyze the scaling of energy transfer efficiency from beam to laser with pulse position, central frequency, and chirp. Dephasing is avoided by using a tailored plasma density profile [1]. The simulations suggest that PWPA is more efficient for positively chirped pulses than negatively chirped or unchirped pulses. The simulations also demonstrate that positively chirped witness pulses yield final laser pulses with a shorter duration and smaller bandwidth. Equations of motion for perturbed quasi-photons in a dephasingless plasma wakefield photon accelerator are derived in the geometric optics approximation [2]. The theoretical quasi-photon trajectories are compared to the PIC simulations.

- [1] R. T. Sandberg and A. G. R. Thomas, Phys. Rev. Lett. 130, 085001 (2023).
- [2] Mendonca, J.T. (2000). Theory of Photon Acceleration (1st ed.). CRC Press. https://doi.org/10.1201/9780367801472

Streak Camera Characterization at the OMEGA-60 Laser Facility *

Kwyntero Kelso ^a, Nicholas Pelepchan ^b, Steven Ivancic ^b, Sean Regan ^b and Carolyn Kuranz ^a

(a) University of Michigan, Center for Laboratory Astrophysics (kkelso@umich.edu)(b) University of Rochester, Laboratory for Laser Energetics

We present preliminary results of the refurbishment and characterization of an x-ray streak camera used at the OMEGA Laser Facility. An x-ray streak camera collects time-resolved x-ray signal with picosecond resolution to characterize the behavior of continuous and pulsed x-ray sources, which are commonly used in high-energy-density science experiments. To repair the deflection plate pulse network, we impedance matched the coaxial divider lines with a nanosecond pulse generator and oscilloscope. We determined the best solution is a 50-50 coaxial split with Laboratory for Laser Energetics manufactured 100Ω semi-rigid coaxial lines. Then we measured the charge-coupled device output using two photon sources, a Hg(Ar) lamp and a 4ω (~1 watt) 10 ns FWHM laser. The simulated cutoff voltage for this design is +-300V. These predicted results were then compared and confirmed with Diagnostic Ten-Inch-Manipulator tests. We used the measured deflection plate pulse and monitor trace to develop a signal processing filter, which allows for accurate deflection plate pulse reconstruction. This algorithm simulated expected signal of the monitor trace for the impedance network. A Bessel filter is applied to the monitor trace to reduce the statistical noise of the pulse. This algorithm was implemented into the shot data processing script used by the OMEGA facilities.

* This work is funded by the U.S. Department of Energy NNSA Center of Excellence under cooperative agreement number DE-NA0004146.

This material is based upon work supported by the Department of Energy [National Nuclear Security Administration] University of Rochester "National Inertial Confinement Fusion Program" under Award Number(s) DE-NA0004144.

Abstracts: Poster Session III

MHD-AEPIC Coupled Fluid-Kinetic Simulations of Dipolarization Fronts in Mercury's Nightside Magnetosphere

Alexander T. Cushen a, Xianzhe Jia a, James Slavin a, Weijie Sun b, Gabor Toth a, and Yuxi Chen a

(a) Department of Climate and Space Sciences, University of Michigan (atcushen@umich.edu)
(b) Space Sciences Laboratory, University of California, Berkeley

Mercury's magnetosphere shares many properties with Earth's but operates on a smaller spatial and temporal scale given its weaker intrinsic field and intense solar wind environment. Hermean substorms, occurring on the timescale of minutes, lead to the accumulation of magnetic flux in the planet's tail lobes, which is ultimately released through nightside reconnection events. These bursty reconnection events eject plasmoids down the magnetotail and dipolarization fronts towards the planet. Prior simulation and observational studies using data from the MESSENGER spacecraft have illustrated how dipolarization fronts preferentially occur in the post-midnight sector, where they travel towards the planet before braking and diverting due to the strong magnetic pressure near the surface [1,2]. However, little is known about the broader role of dipolarization fronts in the Hermean magnetosphere, including their contribution to low-altitude enhanced field regions observed by MESSENGER, current closure of the substorm current wedge, and the quasi-adiabatic compression of the plasma on the closed, dipolarized flux tubes in the braking process. Since the leading edge of the fast sunward plasma bursts are typically on the scale of the ion inertial length, an ideal magnetohydrodynamic approach cannot account for these dynamics.

Using the University of Michigan's Magnetohydrodynamics with Adaptively Embedded Particle-In-Cell (MHD-AEPIC) model with the PIC region in the nightside, we present simulations of Mercury's magnetosphere under a range of solar wind conditions encountered by the planet during its eccentric orbit to study the evolution of dipolarization fronts in the current sheet. We investigate the relationship between the dipolarization front field strength, particle temperature anisotropy, and bulk velocity to establish a quantitative understanding of their propagation. We compare the magnetic flux and current content of the dipolarization fronts to the magnitudes needed to account for the observed magnetic field enhancements near the nightside surface. These results help contextualize the magnetic field and charged particle observations of dipolarization fronts and connect these rapid dynamics in Mercury's current sheet to the formation of a substorm current wedge and sustained dipolarization near the nightside surface.

References

[1] R. M. Dewey, J. A. Slavin, J. M. Raines, A. R. Azari, and W. Sun, JGR: Space Physics. **125**(9), (2020). [2] Y. Chen, G. Tóth, X. Jia, J. A. Slavin, W. Sun, S. Markidis, T. I. Gombosi, and J. M. Raines, JGR: Space Physics. **124**(11), (2019).

Bremsstrahlung Emission in Strongly Coupled Plasmas *

Julian Kinney, Scott Baalrud, Heath LeFevre and Carolyn Kuranz

University of Michigan - Department of Nuclear Engineering and Radiological Sciences (julkin@umich.edu)

The bremsstrahlung process is an important mechanism for radiation transport in astrophysical, fusion, and industrial plasmas. Plasmas created in these systems can often be in an intermediate coupling regime, where the average kinetic energy of particles is on the order of the potential energy at the average interparticle spacing. In this work we present mean force emission theory, which extends the classical theory of bremsstrahlung emission to strongly coupled plasmas. Mean force emission theory utilizes a classical framework where only electron-ion interactions contribute to the emission spectrum. For emission much greater than the plasma frequency, we show that the radiation spectrum can be described by solving for the electron trajectory during a binary collision, but where the electron-ion interactions occur through the potential of mean force. For emission near and lower than the plasma frequency, we show that the classical spectrum can be described using an autocorrelation formalism that captures the effect of multiple collisions in sequence. First, we benchmark the theory using classical molecular dynamics (MD) simulations of a repulsively interacting two-component plasma (see Figure 1). Next, we extend the theory to attractively interacting systems by using a pseudopotential to model the electronion interaction. In the high frequency limit, the pseudopotential leads to a decay of the emission coefficient in a qualitatively similar way as the repulsive case. The pseudopotential also allows for classically bound states to form in the MD simulations, and this leads to peak in the emission spectrum that is absent in the repulsive case.

* This work is funded by the NNSA Stockpile Stewardship Academic Alliances under grant number DE-NA0004100.

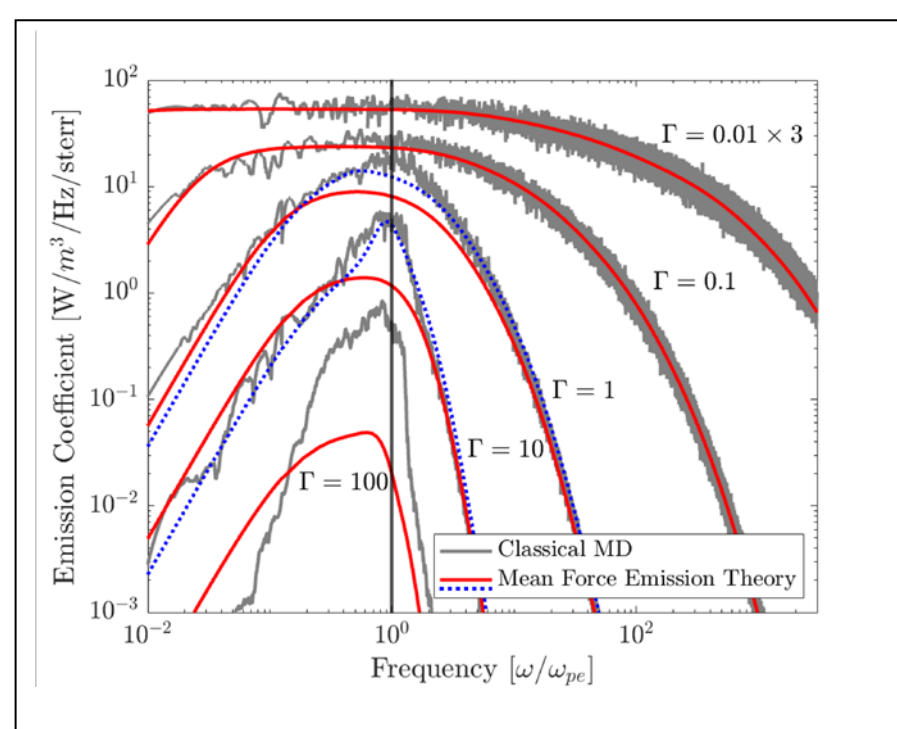


Figure 1 – Calculations of the bremsstrahlung emission coefficient from mean force emission theory compared to MD simulations at different values of the Coulomb Coupling Parameter Γ . Strong coupling occurs when $\Gamma \gtrsim 1$.

Ultrafast Photocarrier Dynamics in CsPbBr₃ Perovskite Microcrystals *

Sheng Lee ^a, Kyeongdeuk Moon ^b, Muhammad Shoaib ^b, Charles N. B. Pedorella ^c, Kellen O'Brien ^c, Meng-Ju Sher ^c, Seokhyoung Kim ^b and Tyler L. Cocker ^a

- (a) Department of Physics and Astronomy, Michigan State University (Leeshen1@msu.edu)
 - (b) Department of Chemistry, Michigan State University
 - (c) Department of Physics, Wesleyan University

We study the ultrafast dynamics of photoexcited charge carriers in micron-scale crystals composed of the inorganic perovskite CsPbBr3 with time-resolved terahertz spectroscopy. Exciting with photon energy close to the band edge, we find that a fast ($<10\,\mathrm{ps}$) decay emerges in the terahertz photoconductivity with increasing pump fluence and decreasing temperature, dominating the dynamics at 4 K. The fluence-

dependent dynamics can be globally fit by a nonlinear recombination model, which reveals that the primary nonlinear recombination mechanism depends on temperature, with Auger scattering determining the fast decay at 77 K but radiative recombination responsible for the fast decay at 4 K. Spectroscopically, the terahertz photoconductivity resembles a Drude response at all delays, yet an additional Lorentz component due to an above-bandwidth resonance is needed to fully reproduce the data.

* Work supported by the Cowen Family Endowment. S. K. acknowledges startup support from the Department of Chemistry at Michigan State University. Research at Wesleyan University is supported by NSF DMR-2316827.

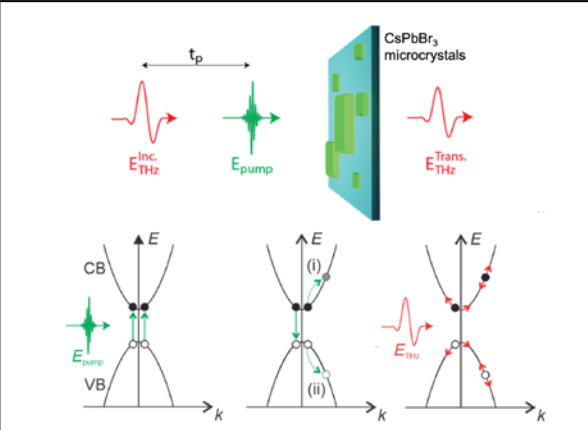


Figure 1 - CsPbBr3 microcrystals grown by chemical vapor deposition with time-resolved terahertz spectroscopy. Optical excitation with photon energy close to the band edge generates a transient photoconductivity that decays non-exponentially on the 10-picosecond timescale at low temperatures, with both Auger and radiative recombination contributing. As the temperature decreases from 77 K to 4 K, the radiative recombination rate is found to increase by three orders of magnitude.

References

[1] S. Lee *et al.* "Temperature-Dependent Recombination Dynamics of Photocarriers in CsPbBr₃ Microcrystals Revealed by Ultrafast Terahertz Spectroscopy," Adv. Opt. Mater. Accepted, (2024).

[2] M. Li *et al.* "Slow Hot-Carrier Cooling in Halide Perovskites: Prospects for Hot-Carrier Solar Cells," Adv. Mater. **31**, 1802486 (2019).

[3] H. Zhang *et al.* "Stable Mott Polaron State Limits the Charge Density in Lead Halide Perovskites," ACS Energy Lett. **8**, 420–428 (2023).

[4] X. Chen *et al.* "Temperature Dependent Reflectance and Ellipsometry Studies on a CsPbBr₃ Single Crystal," J. Phys. Chem. C **123**, 10564 (2019).

[5] P. U. Jepsen *et al.* "Terahertz spectroscopy and imaging – Modern techniques and applications," Laser Photon. Rev. **5**, 124–166 (2011).

[6] R. L. Milot *et al.* "Temperature Dependent Charge-Carrier Dynamics in CH₃NH₃PbI₃ Perovskite Thin Films," Adv. Func. Mater. **25**, 6218–6227 (2015).

Bulk Viscosity of Strongly Coupled Plasmas *

Jarett LeVan and Scott Baalrud

Department of Nuclear Engineering and Radiological Sciences, University of Michigan, Ann Arbor (jarettl@umich.edu)

Bulk viscosity of the one-component plasma (OCP), a model system for strongly coupled atomic plasmas, is computed using molecular dynamics simulations. Using the Green-Kubo formula, we find that the coefficient of bulk viscosity in the OCP is smaller than the shear viscosity for all values of the Coulomb coupling parameter Γ . We also compute bulk viscosity of the rigid rotor one-component plasma (ROCP), a model system for strongly coupled diatomic plasmas. We find that the coefficient of bulk viscosity can exceed the shear viscosity by several orders of magnitude at certain values for Γ and the bond length parameter Ω [1]. This occurs due to the very long rotational relaxation time associated with molecular ions.

Although bulk viscosity is often neglected in plasma modeling, our results suggest that plasmas with a large quantity of molecular ions may have a very large bulk to shear ratio. Including bulk viscosity in fluid simulations may enable more accurate modeling of turbulence, shock waves, and instabilities.

* This work is supported by DOE FES grant No. DE-SC0022201

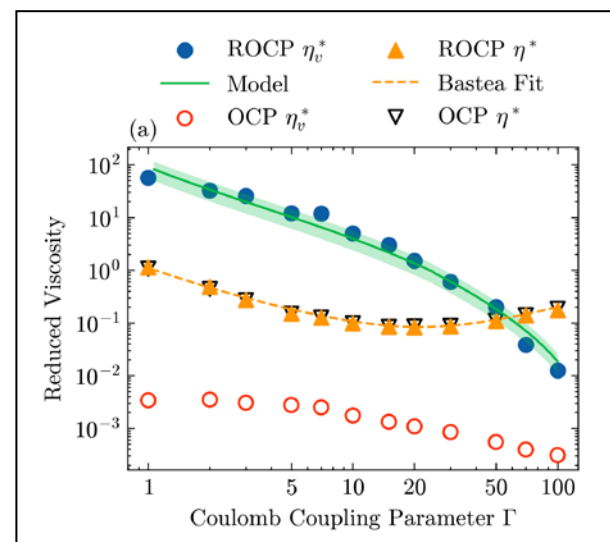


Figure 1 – Reduced coefficient of bulk viscosity (η_v^*) and shear viscosity (η^*) as a function of the Coulomb coupling parameter in the ROCP and OCP.

Reference

[1] LeVan, Jarett, Marco D. Acciarri, and Scott D. Baalrud, "Bulk viscosity of the rigid rotor one-component plasma." Physical Review E **110**.1, 015208 (2024).

Pulsed Low Bias Frequencies for High Aspect Ratio Plasma Etching *

Evan Litch a, Hyunjae Lee c, Sang Ki Nam and Mark J. Kushner b

- (a) Nuclear Engr. & Radiological Sci., University of Michigan, Ann Arbor (elitch@umich.edu)
- (b) Electrical Engr. & Computer Sci., University of Michigan, Ann Arbor (mjkush@umich.edu)
 - (c) Mechatronics Research, Samsung Electronics Co., Ltd., Republic of Korea (hj0928.lee@samsung.com, sangki.j.nam@samsung.com)

Current roadmaps for microelectronics fabrication are focused on fabrication of 3-dimensional devices for higher functionality. Plasma etching steps during fabrication of these 3D devices are becoming increasingly more challenging due to the high aspect ratios (HARs) of the features. For example, 3D-NAND memory structures contain hundreds of alternating layers of SiO₂ and Si₃N₄ requiring etching of vias having aspect ratios (AR) exceeding 100.

Plasma etching of HAR features requires ion energy and angular distributions (IEADs) that are narrow in angle while extending to energies exceeding several kV. These requirements motivate the use of very low frequency biases (VLF) – a few hundred kHz. Trends in the industry are also moving towards pulsed biases to optimize the ratio of radical to ion fluxes. Several challenges arise with the use of pulsed, low frequency, high voltage biases. The thickening of the sheath and charging of focus rings (structures surrounding the wafer) lead to edge exclusion – a region at the edge of the wafer where IEADs are perturbed from their desired, ideal anisotropic properties.

In this presentation, results will be discussed from a computational investigation of IEADs incident onto wafers and remediation of edge exclusion when using pulsed VLF biases in ICPs for etching of trenches for DTI. Simulations were conducted using the Hybrid Plasma Equipment Model (HPEM) [2]. Operating conditions are tens of mTorr mixtures of Ar/Cl₂/O₂ with bias frequencies from 250 kHz to 5 MHz. Bias voltages are up to a few kV with pulse repetition frequencies of up to several kHz. When using continuous wave biases, the charging of the focus ring is sensitive to frequency, and this charging produces sheath curvature at the edge of the wafer, which perturbs IEADs. For example, IEADs are shown in Fig. 1 approaching the edge of a 30 cm diameter wafer for bias frequencies of 250 kHz and 5 MHz for an ICP sustained in Ar/Cl₂/O₂ with bias voltage amplitude of 1 kV. With pulsed biasing, the focus ring is transiently charged both during the VLF cycle and during the pulsed cycle, adding additional challenges to minimizing edge exclusion.

* This work was supported by Samsung Electronics Co. and the US National Science Foundation (2009219).

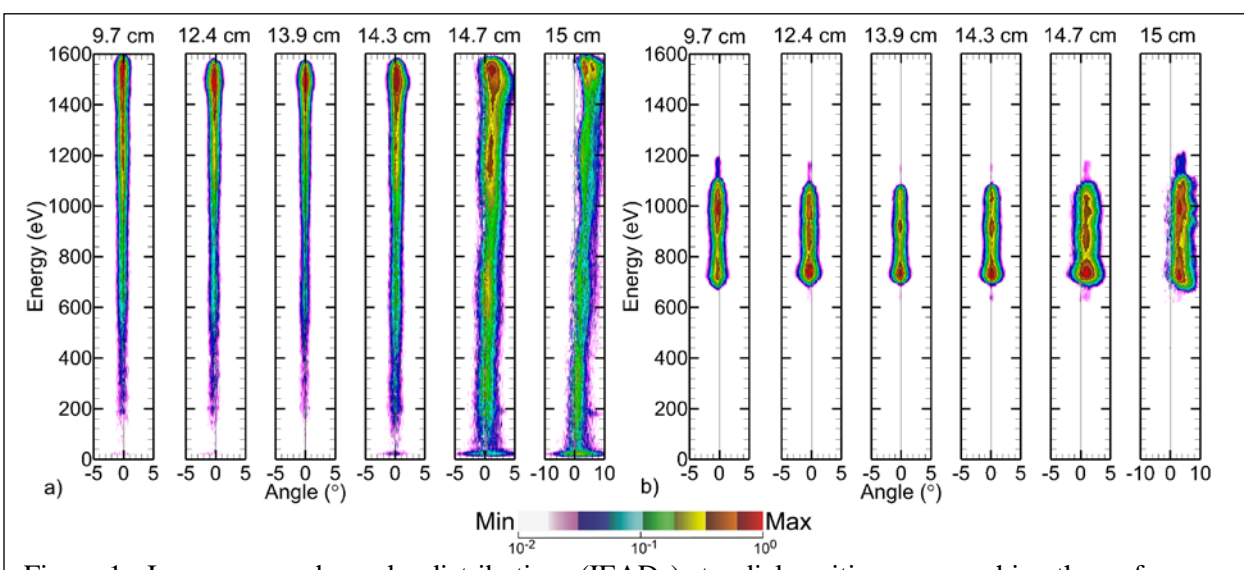


Figure 1 - Ion energy and angular distributions (IEADs) at radial positions approaching the wafer edge for (left) 250 kHz and (right) 5 MHz.

Parametric Analysis of the Beam Kinetic Energy in Linear Beam Devices * Md Wahidur Rahman and Peng Zhang

Michigan State University, East Lansing, MI (rahman63@msu.edu)

Linear beam devices are used for the amplification of microwave which is important to plasma heating, particle acceleration, and fusion research. This work focuses on a high-efficiency RF power amplifier, conducting a parametric analysis of the beam kinetic energy for large signal. The beam kinetic energy is dependent on the gap coupling factor and DC beam perveance [1]. To improve the reliability and efficiency of electron beam systems, it is important to consider space charge effects during beam-circuit

interaction [2,3]. To achieve high conversion efficiency, it is important to minimize the kinetic energy of the beam at the exit of the interaction gap by increasing gap coupling factor and decreasing DC beam perveance.

We calculate the kinetic energy and efficiency of the linear beam device for different beam perveance by injecting different DC beam current. We notice that efficiency of the device is increasing when the beam perveance is decreased [1]. To analyze the normalized kinetic energy (see Fig 1), we study gap coupling factor which is dependent on tunnel and beam radius, gap length, injected RF current, anode voltage, and load resistor. We observe that increasing gap coupling factor lowers the kinetic energy which increases the efficiency of the device [1,2]. Comparing the disk model with and without space charge effects for different beam perveance and gap coupling factor, we find that final kinetic energy of the beam is always higher for with space charge condition due to the presence of the negative charge,

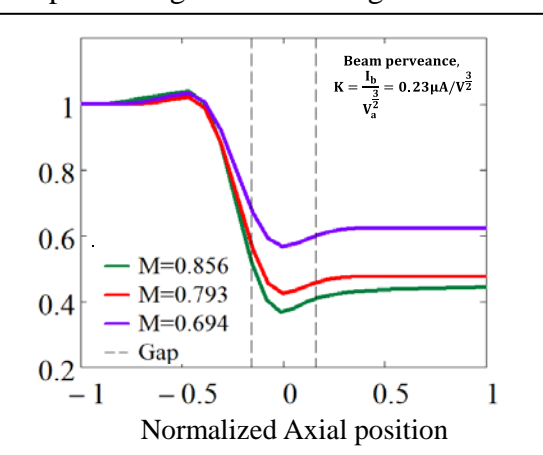


Figure 1 - Normalizad kinectic energy with axial position for different gap coupling factors (M) with space charge considered, where injected RF current = 1.5A, DC beam current = 0.9A, Frequency =1.3GHz, Anode voltage = 25kV, and Load resistor = $26k\Omega$.

indicating a smaller conversion efficiency when considering space charge effects.

* This work is supported by the Office of Naval Research (ONR) YIP Grant No. N00014-20-1-2681, and Air Force Office of Scientific Research (AFOSR) Grant No. FA9550-20-1-0409, and the Air Force Office of Scientific Research (AFOSR) Award No. FA9550-22-1-0523.

- [1] Hechtel, J.R., The effect of potential beam energy on the performance of linear beam devices. IEEE Transactions on Electron Devices **17**(11), pp. 999-1009 (1970).
- [2] R. G. Carter, Microwave and RF Vacuum Electronic Power Sources, 1st ed. Cambridge University Press (2018), doi: 10.1017/9780511979231.
- [3] W. E. Waters, "Space-charge effects in klystrons," IRE Trans. Electron Devices **4**, no. 1, pp. 49–58, Jan. 1957, doi: 10.1109/T-ED.1957.14200.

Measurements of the Dispersion and Growth Rate of Plasma Waves in the Plume of a Hollow Cathode *

Miron Liu and Benjamin Jorns

University of Michigan (mironliu@umich.edu)

Hollow cathodes are commonly employed as both neutralizers and plasma sources for various plasma EP systems. In these devices, the gradients in electric potential and pressure established to drive electron acceleration and gas injection also give rise to the growth of plasma instabilities. Ion acoustic turbulence (IAT), in particular, has been identified as a dominant instability mode influencing ion and electron dynamics in the plumes of hollow cathodes where the growth of these waves has been linked to non-classical resistivity for electrons and anomalous heating of ions [1][2]. It is therefore necessary to account for these non-classical, wave-driven effects in models for accurate simulation of hollow cathodes. However, the direct relationship between IAT, anomalous electron resistivity and ion heating remains

poorly understood. To date, most experimental approaches have used quasilinear theory to relate wave properties to anomalous particle and energy transport, and most simulation efforts have been predicated on strong assumptions about the saturation of these waves [3][4]. While these efforts have aided in the explanation of key trends observed in the plasma state, the description of these instability processes remains incomplete. To achieve a comprehensive understanding of how IAT drives anomalous particle and energy transport, we must first characterize the rate at which these waves extract energy from plasma (i.e. linear growth) and the mechanisms that lead to the saturated energy spectra (i.e. non-linear growth). Direct measurements of these properties, with few exceptions, have proven to be prohibitively difficult to date [2]. With that said, there has been recent work by Brown and Jorns demonstrating the ability to use two-probe correlation techniques to directly infer both the linear and nonlinear growth rates in low temperature plasmas at small scales seen in hollow cathodes [5]. The goal of this work is to demonstrate this technique, modified by the application of Bayesian inference, on a hollow cathode plasma.

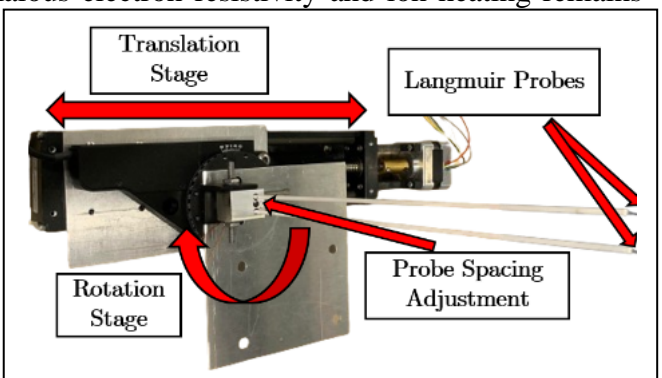


Figure 1 - Wave probe diagnostic for inferring key wave properties.



Figure 2 - LaB₆ hollow cathode test article.

* Work supported by NASA Space Technology Graduate Research Opportunity (NSTGRO) and Rackham Merit Fellowship (RMF).

- [1] A. L. Ortega, B. A. Jorns, and I. G. Mikellides, J. Propul. Power **34**, 1026–1038 (2018).
- [2] B. A. Jorns, I. G. Mikellides, and D. M. Goebel, Phys. Rev. 90, 063106 (2014).
- [3] M. P. Georgin and B. A. Jorns, PSST 29, 2389 (2020).
- [4] B. A. Jorns, C. Dodson, D. M. Goebel, and R. Wirz, Phys. Rev. 96, 023208 (2017).
- [5] Z. A. Brown and B. A. Jorns, Phys. Plasmas 26, 2389 (2019).

Plasma Enhanced Atomic Layer Deposition of Hydrogen Free In₂O₃ Thin Films with High Charge Carrier Mobility *

Sudipta Mondal, Ian Campbell and Ageeth Bol

Department of Chemistry, University of Michigan, Ann Arbor (sudiptam@umich.edu)

In₂O₃ has recently emerged as an alternative channel material for field effect transistors (FETs), owing to its exceptional carrier mobility preservation even when scaled down to ultra-thin layers below 10 nm.[1] Despite the superior performance of In₂O₃-based understanding the underlying operation mechanisms is incomplete, particularly concerning the impact of native defects and doping. Hydrogen dopants in metal oxide films are often responsible for increased Hall mobility, albeit at the detriment of device stability. Herein, we have used plasma-enhanced atomic layer deposition (PEALD) to deposit highly uniform and conformal In₂O₃ thin films. A β-diketonate indium precursor tris(2,2,6,6-tetramethyl-3,5-heptanedionato) indium-(III), which is stable over a large temperature range was used as the indium source. O₂ plasma was selected for oxygen incorporation instead of hydrogen-

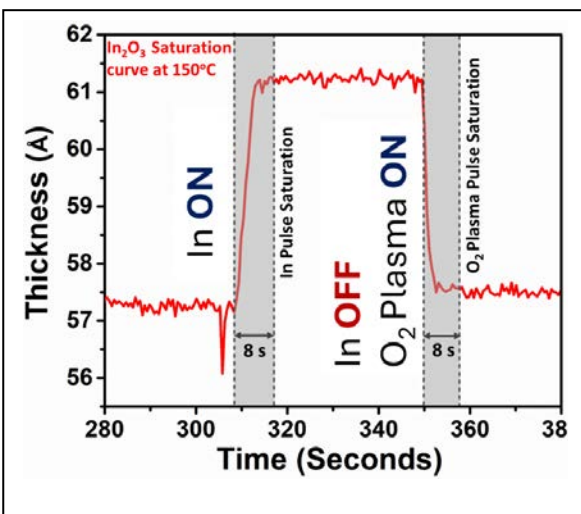


Figure 1 – Saturation Behaviour of In_2O_3 at $150^{\circ}C$ studied using in-situ ellipsometry.

containing precursors like H₂O to prevent unintentional hydrogen doping, while still aiming for high carrier mobility. Saturation behaviour for the PEALD process was studied using in-situ spectroscopic ellipsometry (Figure 1) and indicated a wide ALD window from 150°C to 500°C. Our optimized process achieves a growth rate of 0.14 Å/cycle at 150°C, and 0.29 Å/cycle at 500°C. The In₂O₃ films manifest in a polycrystalline Bixbyite cubic phase, as confirmed by grazing incidence X-ray diffraction (GIXRD). The chemical composition of the films was investigated using X-ray photoelectron spectroscopy (XPS), which revealed a rising number of oxygen vacancies with increasing deposition temperature. Diverse analytical methods, including UV-vis spectroscopy, scanning electron microscopy (SEM), and Hall measurements, were employed to elucidate the influence of oxygen vacancies on the film properties. Our n-type In₂O₃ films showed a Hall mobility value of 84.1 cm²/V-s at a deposition temperature of 150°C, which is among the highest reported for ALD In₂O₃ thin films, making them an ideal candidate as a channel material in FET devices. Through Elastic Recoil Detection Analysis (ERDA), we have excluded the presence of hydrogen dopants by comparing the relative hydrogen concentration in the substrate and the sample, (detection limit ≥ 0.01 atomic %), cementing the role of oxygen vacancies as the principal contributor to the exceptional electrical behaviour in our films. Moreover, we explored post-deposition annealing in air and argon atmospheres as a strategy to modulate oxygen vacancies and, by extension, the electrical properties of the films. We observed that air annealing increases resistivity by eliminating oxygen vacancies, while vacuum annealing enhances conductivity by creating oxygen vacancies.

Reference

[1] Si, M., Hu, Y., Lin, Z., Sun, X., Charnas, A., Zheng, D., Ye, P. D. Nano Lett. 21 (1), 500–506 (2021).

^{*} Work supported by the NWO VICI Grant.

Effects of a Series Resistor on Quantum Tunneling Current in a Dissimilar Metal-Insulator-Metal Nanogap *

Bingqing Wang ^a, Sneha Banerjee ^b and Peng Zhang ^a

(a) Department of Electrical and Computer Engineering, Michigan State University, East Lansing, Michigan, 48824-1226, USA (pz@egr.msu.edu)

(b) Sandia National Laboratories, Albuquerque, NM 87123

In this work, we utilize the model developed by Zhang and Banerjee^{1,2} to analyze current tunneling

in a dissimilar MIM nanogap connected with a series resistor R, driven by a DC voltage V. A series resistor is often added to improve the stability³ of the current and reduce the abrupt rise in current density. However, the addition of a series resistor also leads to an elevated operating voltage requirement, reducing the efficiency and increasing cost⁴. In nanodevices, the necessary interconnects of the circuits inevitably introduce a parasitic series resistance to the device.

In order to delineate the conditions under which the series resistor significantly influences device performance, a comprehensive analysis for tunneling current across a wide range of input parameters is performed. Our findings reveal that the effects of insulator properties, electrode work functions, and bias voltage are critical in determining the forward and reverse bias tunneling currents. Particularly, the impact of the series resistor becomes pronounced in configurations with small insulator thicknesses and high voltages, where the junction impedance is comparable to the resistor value. As resistance increases, the asymmetry between the forward and reverse bias currents diminishes, indicating a shift toward an ohmic behavior of the tunneling gap.

* The work is supported by the Air Force Office of Scientific Research (AFOSR) Award No. FA9550-22-1-0523.

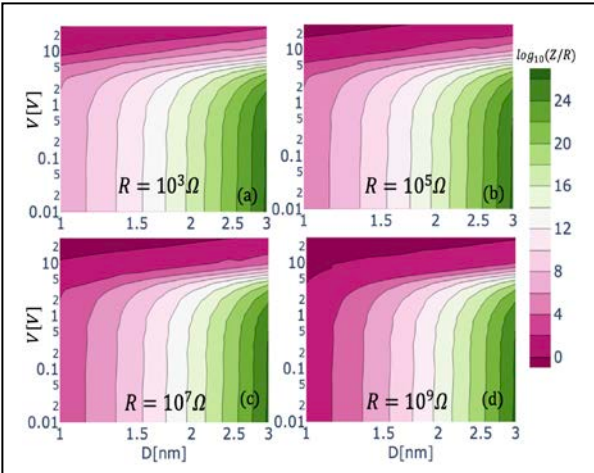


Figure 1 Contour plots illustrating logarithmic scale of impedance (Z) normalized resistance (R) across varying distance(D) and circuit voltages (V). Each panel corresponds to a different fixed resistance value, with (a) $R = 10^3 \Omega$, (b) $R = 10^5$ Ω , (c) R = $10^7 \Omega$, and (d) R = $10^9 \Omega$. The horizontal axis of each plot represents the gap distance from 1 nm to 3 nm, while the vertical axis shows the voltage range from 0.01 V to 20 V. The log-scale color gradients represent the impedance normalized by the respective resistance values, transitioning from low (green) to high (pink) values.

- [1] S. Banerjee and P. Zhang, AIP Advances 9, 085302 (2019).
- [2] P. Zhang, Scientific reports 5, 9826 (2015).
- [3] J. D. Levine, Journal of Vacuum Science & Technology B 14, 2008–2010 (1996).
- [4] J. W. Luginsland, A. Valfells, and Y. Y. Lau, Applied physics letters 69, 2770–2772 (1996).

Investigating Solar Wind Formation and Propagation via Entropy Cross-correlation Analysis

Aidan Nakhleh a, Nicholeen Viall b, Susan Lepri a, and Jim Raines a

(a) University of Michigan (naidan@umich.edu, slepri@umich.edu, jraines@umich.edu) (b) NASA Goddard Space Flight Center (nicholeen.m.viall@nasa.gov)

The solar corona supplies and accelerates the supersonic solar wind that propagates through and interacts with the solar system [1]. To study how different regions of the solar corona form and accelerate the solar wind, we are investigating the specific proton entropy of the solar wind and how this entropy correlates with elemental composition data collected by the Advanced Composition Explorer (ACE) SWEPAM and SWICS instruments from 1998-2001. It is known that elemental compositions can act as tracers of coronal physics, such as the first ionization potential (FIP) fractionation effect represented by the abundance ratio of Iron to Oxygen. The FIP effect details particle ionization and acceleration in the partially ionized chromosphere and low corona ($R < 0.01R_{\odot}$) [2]. The ratio of densities between different charge states of ionized carbon or oxygen (i.e. C^{6+}/C^{5+} or O^{7+}/O^{6+}) constrains electron densities, wind expansion profiles, and the lower to middle coronal temperature environment $(R > 0.5R_{\odot})$ via the characteristic freeze-in effect [3]. By treating solar wind protons as an adiabatically expanding gamma-law gas with specific entropy $S \sim \ln(\frac{T}{nY-1})$, we cross correlate this quantity with elemental compositions to study whether entropy is influenced by physics determining electron thermalization in the low-mid corona and if it freezes into the solar wind like $0^{7+}/0^{6+}$ does, or if entropy is governed by MHD wave physics in the chromosphere like Fe/O is. This cross-correlation analysis allows us to study the physics that gives the solar wind its entropy, and how that entropy evolves as the solar wind advects into the heliosphere. This investigation provides a new means to study the structure of the solar corona and how it produces the solar wind in the evolving framework of understanding, which is of interest to the heliophysics and space weather communities.

- [1] Parker, Eugene N. Astrophysical Journal **128**, p. 664 128 (1958).
- [2] Laming, J. Martin. Living Reviews in Solar Physics 12, 1-76 (2015).
- [3] Hundhausen, A. J., H. E. Gilbert, and S. J. Bame. Astrophysical Journal 152, p. L3 152 (1968).

Investigation of Plasma Gratings as a Diagnostic for Low Temperature Plasmas

Bilal Hassan and Christopher M. Limbach

Department of Aerospace Engineering, University of Michigan (bilalhsn@umich.edu, limbach@umich.edu)

Experimental characterization of the electron velocity distribution function (EVDF) at relevant temporal and spatial scales remains a challenge for conventional laser diagnostics, such as Scattering, due to low signal levels under typical low temperature plasma (LTP) conditions. The present work aims to evaluate the potential utilization of scattering from transient plasma gratings as a diagnostic for measuring spatially and temporally resolved EVDFs. This work considers both the formation and decay of plasma gratings in non-magnetized LTPs produced by pondermotive forcing in crossed femtosecond or picosecond pump beams. The plasma grating dynamics are investigated using 1D1V kinetic simulations with a frozen ion background. The spatiotemporal evolution of the EVDF is simulated in a semi-Lagrangian framework with the BGK operator accounting for collisions in the weakly ionized plasma. Light scattering from a temporally delayed probe beam is computed by numerical beam propagation within the slowly varying envelope approximation. Numerical results are presented over a range of plasma conditions, grating formation conditions, and scattering parameters as characterized by key dimensionless parameters. These results further motivate the design of experiments capable of realizing single shot characterization of the EVDF and other plasma parameters. This work was previously presented at GEC 2024, and is attached below.

- [1] Benjamin Vincent, Sedina Tsikata, George-Cristian Potrivitu, and Stephane Mazoure. Incoherent Thomson scattering diagnostic development for plasma propulsion investigations. IEPC-2017, (442).
- [2] E B Cummings. Laser-induced thermal acoustics: simple accurate gas measurements. Optics letters **19**(17):1361–1363 (1994).
- [3] L. M. Gorbunov and A. A. Frolov. Collision of two short laser pulses in plasma and the generation of short-lived Bragg mirrors. Journal of Experimental and Theoretical Physics, **93**(3):510–518 (2001).
- [4] Mokrov, Mikhail, Mikhail N. Shneider, and Alexandros Gerakis. "Analysis of Coherent Thomson Scattering from a Low Temperature Plasma." Physics of Plasmas **29**, no. 3.
- [5] Hans Joachim Eichler, Peter Gunter, and Dieter W. Pohl. Laser-Induced Dynamic Gratings, Springer Berlin, Heidelberg, 1st ed. (2013).

Characterizing ExB Plasmas with Time-Resolved Thomson Scattering *

Parker J. Roberts and Benjamin A. Jorns

Department of Aerospace Engineering, University of Michigan (pjrob@umich.edu)

Devices which rely on the confinement of low-temperature plasmas for their operation are subject to the effects of plasma turbulence and oscillations. For example, the space propulsion devices known as Hall thrusters, which use an annular ExB plasma to accelerate ions, exhibit high sensitivity to plasma oscillations in terms of their performance and lifetime [1]. Both microscopic plasma instabilities and large-scale global modes affect the operation of these devices in non-classical ways. In order to model and design these thrusters and other ExB plasma devices from first principles, it is therefore necessary to characterize their time-resolved electron dynamics.

To measure the electron properties, we leverage recent advancements in incoherent Thomson scattering that have enabled the application of this

scattering that have enabled the application of this diagnostic to low-density plasmas [2,3]. These techniques are inherently time-averaged due to their low signal strength, leading to the need to perform ensemble averaging on measurements. In this study, however, we leverage machine learning algorithms to learn mappings from measurements of the global plasma state, such as the discharge current, to the noisy Thomson scattering signal. This allows us to reconstruct and denoise the signal of interest as a function of the oscillation phase.

We present measurements using this method in the plume of the H9 Hall thruster operating on krypton propellant. We acquire the time-resolved EVDF and from this compute the time-resolved plasma properties, such as density, temperature, and ExB drift speed. We combine this data with laser-induced fluorescence measurements of the ions to create a framework for describing anomalous electron momentum transport as a function of time and space. This inference feeds directly into modeling efforts aimed at capturing the

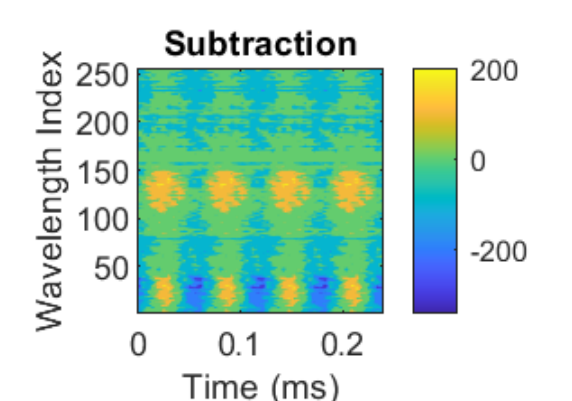


Figure 1 – Evolution of the EVDF measured by Thomson scattering during intense "breathing mode" oscillations in a high-power Hall thruster. This initial low-signal phase portrait was acquired during a pathfinding experiment, and at this operating condition the EVDF fades in and out of visibility due to electron density fluctuations.

time-resolved thruster dynamics and make predictions about performance and lifetime from first principles.

* Work supported by the Air Force Office of Scientific Research through a DURIP grant, and by NASA through a NASA Space Technology Graduate Research Opportunity as well as the Joint Advanced Propulsion Institute, a Space Technology Research Institute.

- [1] J. P. Boeuf and L. Garrigues, J. Appl. Phys. 84, 3541-3554 (1998).
- [2] B. Vincent et al., Plasma Sources Sci. Technol. 27, 055002 (2018).
- [3] P. J. Roberts and B. A. Jorns, Phys. Rev. Lett. 132, 135301 (2024).

Maximizing Energy Efficiency in Selective Plasma-Induced Propylene Epoxidation Using Water as the Oxygen Source *

Han-Ting Chen, Dongho Lee, Yi Zhang and Suljo Linic

Department of Chemical Engineering, University of Michigan, Ann Arbor, Michigan 48109 (hantingc@umich.edu)

Propylene oxide (PO) is used in niche applications that do not require high volumes and concentrations, such as a fumigant and disinfectant for food,[1] a sterilizer for medical equipment,[2] and as an agent for modifying food products like starch and alginate.[3] These applications, coupled with the high transport and storage costs due to the toxic nature of PO, create a strong incentive to develop PO production strategies tailored for smaller-scale and on-site productions, rather than relying on centralized mass production and long-term storage

Herein, we designed a plasma-induced catalytic process using only water and propylene (C₃H₆) as reactants to form PO. In the plasma phase, water is converted into hydrogen peroxide (H₂O₂), which is then transferred into the liquid phase. H₂O₂ serves as an

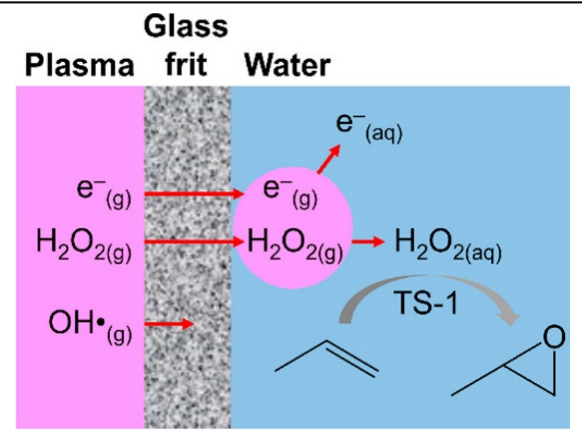


Figure 1 – Hydrogen peroxide transfers from the plasma phase to the liquid phase, driving the partial oxidation of propylene to propylene oxide.[4]

oxidizing agent to epoxidize the dissolved C₃H₆ over a titanium silicate-1 (TS-1) catalyst dispersed in the solution. A glass frit was added between the plasma and liquid phase to suppress the formation of deep oxidation products (i.e., CO₂), achieving a carbon-based selectivity of more than 98%. Additionally, the influence of plasma parameters, such as plasma duration and voltage, on the activity and energy efficiency of PO production was investigated. Through experiments and simulations, we identified that optimizing plasma parameters is essential for maximizing PO production per unit of energy input. These findings present a method for on-demand PO production with high energy efficiency using only C₃H₆ and water, making it suitable for various specialized applications.

* Work supported by Army Research Office and was accomplished under Grant No. W911NF-20-1-0105.

- [1] M. D. Danyluk, A. R. Uesugi, and L. J. Harris, J. Food Protect **68**, 1613 (2005).
- [2] H. Sato, T. Kidaka, and M. Hori, Int. J. Artif. Organs 8, 109 (1985).
- [3] Propylene Oxide Environmental Health Criteria 56; Finland (1985).
- [4] D. Lee, H.-T. Chen, and S. Linic, JACS Au 3, 997 (2023).

Studies of Preheat-induced Mix in MagLIF Targets *

<u>Jaela Whitfield</u> ^a, J. R. Fein ^b, M. R. Gomez ^b, M. R. Weis ^b, A. Harvey-Thompson ^b, J. Fooks ^c, M. Weir ^c, T. Phipps ^c and C. Kuranz ^d

- (a) Department of Applied Physics, University of Michigan (jaecwhit@umich.edu)(b) Sandia National Laboratory(c) General Atomics
- (d) Department of Nuclear Engineering and Radiological Sciences, University of Michigan

Magnetized Liner Inertial Fusion (MagLIF) is an inertial confinement fusion concept that preheats a magnetized fuel prior to compression and has the potential to reach high thermonuclear fusion yields. During the laser preheating stage, the higher-density liner material can blow off the liner wall and mix into the lower-density D2 fuel via x-ray ablation or impact from the late-time blast wave. Adding a magnetic field allows the laser energy to be deposited deeper within the plasma causing the expanded coating to become uniformed. We plan to show preliminary data analysis from a scaled MagLIF experiment executed on Omega to characterize and diagnose the mixing of material from the inner surface of the target preheating stage. We will show density profiles of the liner material and an assessment of possible mixing with the D2 fuel as the laser-generated x-rays and blast wave interact with the liner.

* This work is funded by the U.S. Department of Energy NNSA Center of Excellence under cooperative agreement number DE-NA0003869.

Sandia National Laboratories is a multi-mission laboratory managed and operated by National Technology & Engineering Solutions of Sandia, LLC., a wholly owned subsidiary of Honeywell International, Inc., for the U.S. Department of Energy's National Nuclear Security Administration under contract DE-NA0003525.

Mechanisms for Cryogenic Plasma Etching

Yeon Geun Yook and Mark J. Kushner

Department of Electrical Engineering and Computer Science, University of Michigan (ygyook@umich.edu, mjkush@umich.edu)

The increasing demands for high-aspect-ratio (HAR) plasma etching for 3-dimensional devices have produced a resurgence in innovations in cryogenic plasma etching (CPE). CPE is a process in which the substrate, in an otherwise conventional capacitively coupled plasma or inductively coupled plasma, is cooled temperatures as low as –90 °C. The lower substrate temperature is thought to increase the rate of adsorption of precursor species to the degree of having a thin condensed layer. CPE has demonstrated significantly higher etch rates than conventional methods for aspect ratios over 100, though the mechanisms remain unclear. Key gas mixtures, such as those producing HF and H₂O, are believed to form a hydrofluoric acid layer, typically causing isotropic etching. However, lower temperatures suppress this, allowing anisotropic etching via ion bombardment. In gas mixtures that do not contain, for example, fluorocarbon species there is not a natural source of passivation for sidewall control, which suggests that passivation is in the form of etch products.

In this presentation, results will be discussed from a computational investigation of CPE of SiO₂ on

reactor and feature scales using the Hybrid Plasma Equipment Model (HPEM) and Monte Carlo Feature Profile Model (MCFPM). The processing condition is inductively coupled plasma of tens of mTorr pressure with bias voltage source. An investigation of surface kinetics during CPE was first performed using fluxes derived from the reactor scale simulation. The consequences of adsorption probabilities, redeposition of etch products and enhanced yield on etch rate and profile control will be discussed. Results for coupled reactor and feature scale simulations for CPE of SiO₂ using CF₄/H₂/Ar and HF/Ar mixtures will then be

discussed with the goal of determining whether these

proposed mechanisms are consistent with practice in

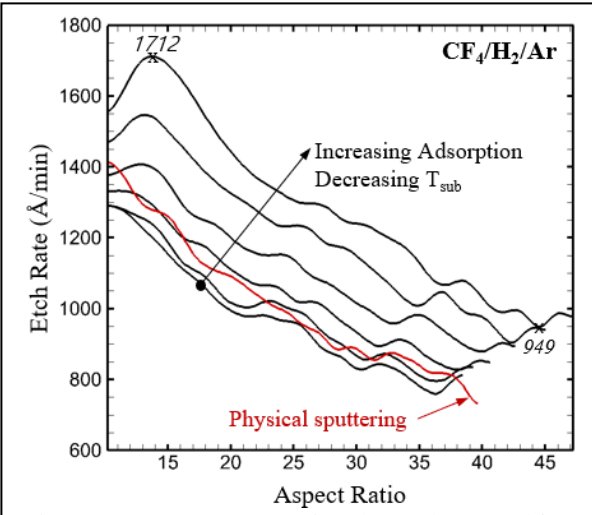


Figure 1 – Aspect ratio dependent etching (ARDE) as a function of substrate temperature in $CF_4/H_2/Ar$ plasma. As the temperature decreases, the etch rate increases, enabling high etch rates even at high aspect ratios.

References

high volume manufacturing.

- [1] Yoshihide Kihara et al., "Beyond 10 μm Depth Ultra-High Speed Etch Process with 84% Lower Carbon Footprint for Memory Channel Hole of 3D NAND Flash over 400 Layers", IEEE Symposium on VLSI Technology and Circuits (2023).
- [2] Shih-Nan Hsiao et al., Small Methods 2024, 2400090 (2024).
- [3] C. R. Helms and B. E. Deal, J. Vac. Sci. Technol. A 10, 806-811 (1992).

Fluid Model Performance Predictions of a Coaxial Rotating Magnetic Field Thruster *

Grace Zoppi, Tate Gill, Christopher Sercel and Benjamin Jorns

Department of Aerospace Engineering, University of Michigan (gzoppi@umich.edu)

The Rotating Magnetic Field (RMF) thruster operates as a type of inductively coupled plasma thruster. This method of energy transfer enables operational regimes of high-power densities and electrodeless designs. Both benefits serve as key enabling features for the next generation of electric propulsion. Specifically, high power densities facilitate favorable scaling to higher powers, and electrodeless designs allow for the use of alternative propellants without concerns of cathode poisoning. The RMF thruster, in particular, retains these architectural advantages without requiring high voltages and currents, as thrust production is proportional to the frequency of the RMF. However, to date, at the University of Michigan's Plasmadynamics and Electric Propulsion Laboratory overall performance has remained low, at less than 3% efficiency [1]. To ultimately enhance thruster performance, we developed a neutral-plasma species steady state fluid model to distinguish between dominate loss mechanisms [2]. Using experimental data measurements of thrust and power coupled into the plasma, we calibrated the fluid model to a conical 5kW test article. We then leveraged the calibrated model to globally optimize thruster efficiency. This optimization indicated that higher RMF and applied radial field strengths are key contributors to improved performance, leading to the development of a new RMF coaxial design rather than the previous conical configurations. To streamline the design process, we repurposed a 6kW Hall thruster by replacing its inner and outer screens with RMF antennas housed in structural ferrite shells. This arrangement strengthens the RMF in the channel region, and the closer spacing between antenna pairs further enhances the field compared to the conical V3 thruster design. The new geometry necessitated updates to the RMF thruster fluid model. After making these updates, we ran an optimizer to determine the applied field strengths, neutral flow rate, and input power needed to maximize overall thruster efficiency bounded by these new geometric constraints.

* Work supported by NASA Grant 80NSSC24K1334.

References

[1] T. Gill, C. Sercel, G. Zoppi, and B. Jorns, "A Comparative Study of Continuous-Wave and Pulsed Operation of Rotating Magnetic Field Thrusters for Plasma Propulsion," AIAA SCITECH 2024 Forum (2024). https://doi.org/10.2514/6.2024-2706.

[2] G. Zoppi, T. Gill, C. Sercel, and B. Jorns, "Efficiency Mode Analysis of a Continuous Wave Rotating Magnetic Field Thruster Informed by a Validated Fluid Model," in 38th International Electric Propulsion Conference, 2024. IEPC Paper 2024-761.

List of Participants

First name	Last name	Email	University
Madison	Allen	mgallen@umich.edu	U-M
Andre	Antoine	aantoine@umich.edu	U-M
Lucas	Babati	lbabati@umich.edu	U-M
Adam	Bedel	abedel@umich.edu	U-M
Kimberly	Beers	kimbeers@umich.edu	U-M
Neil	Beri	nebe@umich.edu	U-M
Declan	Brick	brickd@umich.edu	U-M
Khalil	Bryant	kalelb@umich.edu	U-M
Han-Ting	Chen	hantingc@umich.edu	U-M
Veronica	Contreras	vacontre@umich.edu	U-M
Vivian	Cribb	vcribb@umich.edu	U-M
Alexander	Cushen	atcushen@umich.edu	U-M
Connor	DiMarco	cdimarco@umich.edu	U-M
Ari	Eckhaus	aeckhaus@umich.edu	U-M
Md Arifuzzaman	Faisal	faisalmd@msu.edu	MSU
Sarah	Feldman	sarfeldm@umich.edu	U-M
Sarah	Frechette Roberts	rober964@msu.edu	MSU
Yifan	Gui	evangyf@umich.edu	U-M
Michael	Hackett	mthacket@umich.edu	U-M
Bilal	Hassan	bilalhsn@umich.edu	U-M
Yves	Heri	heriyves@msu.edu	MSU
Chenyao	Huang	chenyaoh@umich.edu	U-M
Isaac	Huegel	idhuegel@umich.edu	U-M
William	Hurley	wjhurley@umich.edu	U-M
Jisu	Jeon	jisujeon@umich.edu	U-M
Lan	Jin	jinlan1@msu.edu	MSU
Kwyntero	Kelso	kkelso@umich.edu	U-M
Julian	Kinney	julkin@umich.edu	U-M
Sheng	Lee	leeshen1@msu.edu	MSU
Jarett	LeVan	jarettl@umich.edu	U-M
Evan	Litch	elitch@umich.edu	U-M
Miron	Liu	mironliu@umich.edu	U-M
Md.	Mashrafi	mashrafi@msu.edu	MSU
Sudipta	Mondal	sudiptam@umich.edu	U-M
Aidan	Nakhleh	naidan@umich.edu	U-M
Tanvi	Nikhar	nikharta@msu.edu	MSU
Braden	Oh	bradenoh@umich.edu	U-M
Md Wahidur	Rahman	rahman63@msu.edu	MSU
Parker	Roberts	pjrob@umich.edu	U-M

First name	Last name	Email	University
Milos	Sretenovic	sretenov@msu.edu	MSU
Bingqing	Wang	wangbi27@msu.edu	MSU
James	Welch	welchjc@umich.edu	U-M
Stephen	White	whites73@msu.edu	MSU
Jaela	Whitfield	jaecwhit@umich.edu	U-M
Xitong	Xu	xuxitong@msu.edu	MSU
Yeon Geun	Yook	ygyook@umich.edu	U-M
Grace	Zoppi	gzoppi@umich.edu	U-M